

FILE COPY
NO. J-W

CASE FILE
COPY

NATIONAL ADVISORY COMMITTEE
FOR AERONAUTICS

TECHNICAL NOTE

No. 1220

EFFECT OF EXHAUST PRESSURE ON THE PERFORMANCE OF
AN 18-CYLINDER AIR-COOLED RADIAL ENGINE WITH
A VALVE OVERLAP OF 40°

By David S. Boman, Tibor F. Nagey
and Ronald B. Doyle

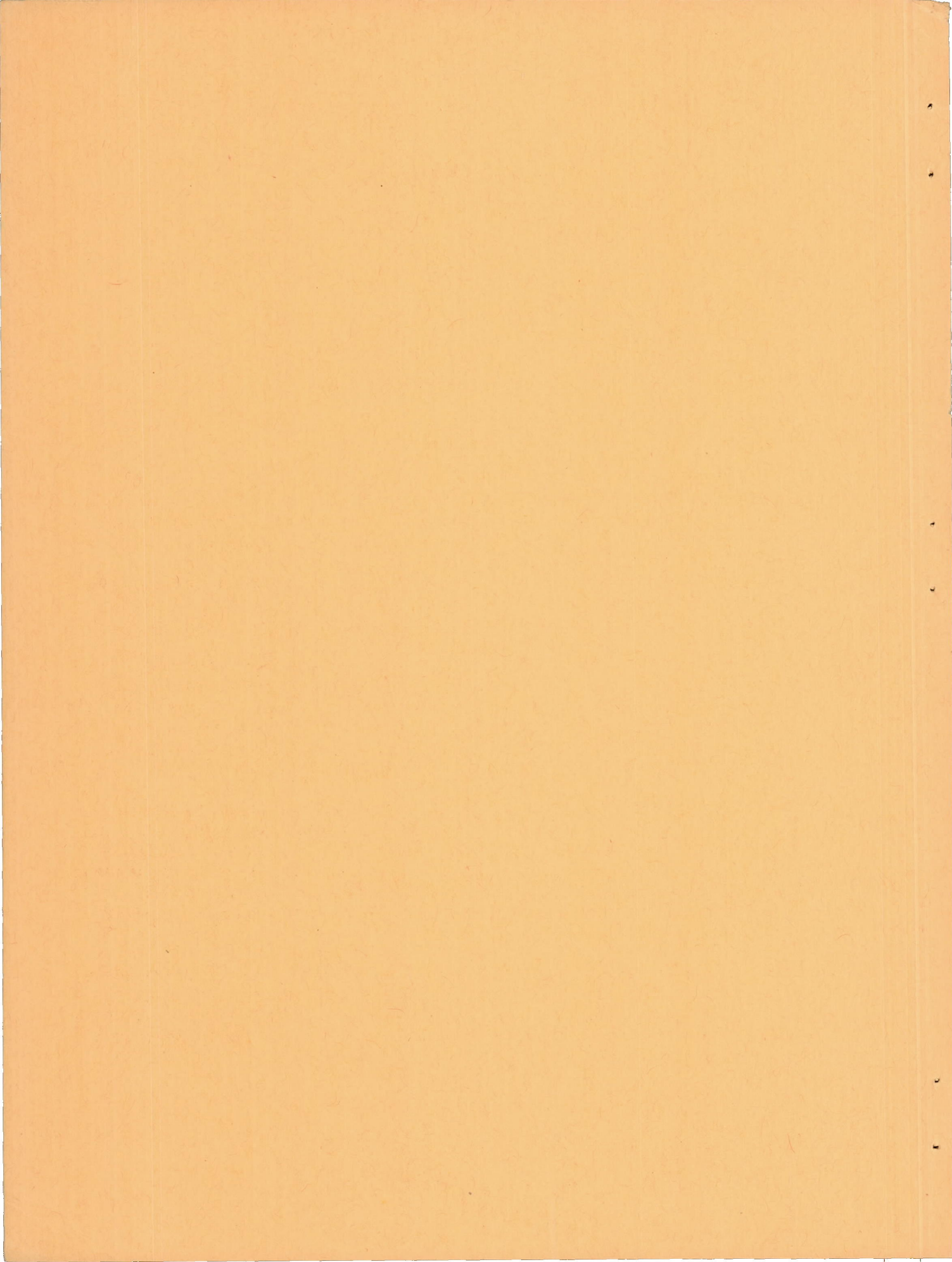
Aircraft Engine Research Laboratory
Cleveland, Ohio



Washington
March 1947

FILE COPY

To be returned to
the files of the National
Advisory Committee
for Aeronautics
Washington, D. C.



TECHNICAL NOTE NO. 1220

EFFECT OF EXHAUST PRESSURE ON THE PERFORMANCE OF
AN 18-CYLINDER AIR-COOLED RADIAL ENGINE WITH
A VALVE OVERLAP OF 40°

By David S. Boman, Tibor F. Nagey
and Ronald B. Doyle

SUMMARY

An investigation was made to determine the effect of exhaust pressure on the performance of an 18-cylinder air-cooled radial engine equipped with a conventional exhaust collector ring. The investigation covered a range of engine speeds from 1200 to 2400 rpm, inlet-manifold pressures from 30 to 45 inches of mercury absolute, and fuel-air ratios of 0.069, 0.085, and 0.100. The exhaust pressure was varied, in general, from approximately 7 inches of mercury absolute to about 20 inches of mercury above the inlet-manifold pressure.

The engine power increased at a diminishing rate as exhaust pressure decreased. For any given engine speed and fuel-air ratio, good correlation of the power over the complete test range of inlet-manifold pressure and exhaust pressure was obtained by plotting the ratio of indicated mean effective pressure to inlet-manifold pressure against the ratio of exhaust pressure to inlet-manifold pressure.

When the ratio of the brake horsepower at any exhaust pressure to the brake horsepower at the same engine speed, fuel-air ratio, and inlet-manifold pressure but at an exhaust pressure equal to inlet-manifold pressure was plotted against the ratio of the exhaust pressure to the inlet-manifold pressure, a single curve resulted for each engine speed regardless of inlet-manifold pressure, exhaust pressure, or fuel-air ratio.

The average cylinder-head temperatures were found to increase as the exhaust pressure increased at constant conditions of fuel-air ratio, engine speed, inlet-manifold pressure, and cooling-air pressure drop. The effect became more marked as the fuel-air ratio decreased from 0.100 to 0.069.

INTRODUCTION

The efficient utilization of the energy in the exhaust gases of an aircraft engine is of importance as a means of obtaining improved power-plant performance. The possibility of improving engine performance by gearing a turbosupercharger to the engine crankshaft is discussed in reference 1. The turbine power in excess of that required for supercharging is available to the propeller. In order to increase the turbine power at a fixed set of engine operating conditions, higher exhaust pressures than atmospheric pressure must be imposed on the engine, which results in a reduction in engine power and charge-air flow. The distribution of power between the engine and the turbine for either minimum specific fuel consumption or maximum net power will depend on the reaction of the brake power and the charge-air flow of the engine to increased exhaust pressures. Reference 2 shows that exhaust pressure has an appreciable effect on engine performance and this effect varies with the particular engine investigated.

A dynamometer investigation was therefore conducted at the NACA Cleveland laboratory to determine the effect of exhaust pressure on the performance of an 18-cylinder air-cooled radial engine with a valve overlap of 40° . The investigation covered a range of engine speeds from 1200 to 2400 rpm, inlet-manifold pressures from 30 to 45 inches of mercury absolute, and fuel-air ratios of 0.069, 0.085, and 0.100. Runs were made with various combinations of the variables and, in general, the exhaust pressure was varied from approximately 7 inches of mercury absolute to about 20 inches of mercury above the inlet manifold pressure. The effect of exhaust pressure on engine power was correlated by two methods: indicated power by the method developed in reference 2 and brake power by a method developed in the present report. Curves are presented that show the effect of exhaust pressure on engine power, charge-air flow, volumetric efficiency, and exhaust-gas temperature.

During this investigation, cooling data were taken and the effect of exhaust pressure on cooling is reported in reference 3.

INSTALLATION AND INSTRUMENTATION

An R-2800-5 (A series) 18-cylinder air-cooled radial engine was used. The engine is rated for take-off at 1850 brake horsepower at an engine speed of 2600 rpm with a maximum continuous rating of 1500 brake horsepower at 2400 rpm with the supercharger in low gear ratio and 1450 brake horsepower at 2400 rpm with the supercharger in high gear ratio. Pertinent specifications of the engine are:

Bore, inches	5.75
Stroke, inches	6.00
Displacement, cubic inches	2804
Compression ratio	6.65
Reduction-gear ratio	2:1
Valve overlap, degrees	40
Spark setting, degrees B.T.C.	25
Impeller diameter, inches	11
Supercharger-gear ratio:	
Low	7.6:1
High	9.45:1

The setup is shown in figures 1 and 2; the engine was rigidly supported on its mounting structure and was connected by an extension shaft to a 2000-horsepower eddy-current dynamometer. Dynamometer torque was measured with a balanced-diaphragm torquemeter of the type described in reference 4. Engine speed was measured with a chronometric tachometer.

Cooling air from the laboratory supply system was delivered to the top of an air box located between the engine and the dynamometer. This box served as a large air reservoir for providing a uniform cooling-air distribution over the front of the engine. The cooling air flowed from the air box through a faired nozzle section, across the engine through the cylindrical engine cowling, and discharged into the room.

The induction system could be augmented by the laboratory combustion-air supply when necessary. A butterfly valve was located in the charge-air pipe between the charge-air orifice and the engine to allow adjustment of the carburetor-inlet pressure to such a value that the desired inlet-manifold pressure (blower-rim pressure) could be obtained with full-open engine throttle. Turning vanes were installed in the pipe ahead of the carburetor in order to insure uniform charge-air distribution at the carburetor top deck. Charge-air flow was measured by a thin-plate orifice installed, according to A.S.M.E. specifications, in the pipe approximately 30 feet upstream of the carburetor.

A needle valve in a line connecting the high-pressure chamber of the carburetor with the fuel nozzle was used to regulate the fuel flow in order to maintain constant fuel-air ratios. The rate of flow of the fuel (AN-F-28, Amendment 2) was measured by a calibrated rotameter.

The exhaust-gas collector ring was the type used in the turbo-supercharger installations on the P-47 airplane and was built in

half-sections, one for each side of the engine. The halves of the collector ring were connected to the laboratory altitude exhaust system through a Y-section of pipe and a 90° mitered elbow. The distance from the junction of the Y-section to the elbow was approximately $2\frac{1}{2}$ feet. The engine exhaust pressure was controlled by throttling the flow of exhaust gases into the exhaust system with a butterfly valve. The engine exhaust pressure was measured by a static-pressure tap located at the section where the exhaust pipe was connected to the exhaust-duct elbow.

The cooling-air total pressure in front of the cylinder heads was measured with three shrouded total-pressure tubes mounted on rakes and placed directly in front of the engine 120° apart and at the same radial distance as the middle circumferential head fin. Three shrouded total-pressure tubes were also mounted on the rakes for measuring cooling-air total pressure in front of the cylinder barrels. These tubes were placed at the same radial distance as the center of the cylinder barrels. The static pressure behind the cylinder heads was measured with an open-end tube placed in the baffle curl of each of the nine rear-row cylinders at the same radial distance as the cylinder-head total-pressure tubes. The static pressure behind the barrels was measured by three static-pressure tubes mounted on rakes behind the rear-row cylinders and at the same radial distance as the barrel total-pressure tubes. All static-pressure tubes were installed in such a position that they received no velocity pressure. The cooling-air pressure drop was taken as the difference between the average total pressure in front of the cylinder heads and the average static pressure behind the heads corrected to sea-level density condition. All pressures were read on manometers.

Exhaust-gas temperatures were measured approximately 18 inches downstream of the junction of the Y-section by three quadruple-shielded chromel-alumel thermocouples located on one circumference and spaced 120°. The depth of thermocouple immersion was approximately three-tenths of the pipe diameter.

The cooling-air temperature was measured by three thermocouples mounted on the total-pressure-tube rakes and was taken as the average of these three thermocouple readings.

Thermocouples were located on each cylinder at the following locations: rear-spark-plug gasket, rear center of barrel, and rear-spark-plug boss. The gasket thermocouples were made by silver-soldering the thermocouple wires into a small hole drilled into the tab to the outer edge of the copper spark-plug gasket. The barrel

thermocouples were embedded in the aluminum barrel mufflers at the rear between the two middle barrel fins. The boss thermocouples were embedded 30 percent of the cylinder-head thickness at a point $45/64$ inch from the spark-plug axis and 45° from the bottom of the spark-plug boss toward the exhaust port. The average cylinder-head temperature was taken as the average of the thermocouple readings at the rear-spark-plug boss.

The carburetor-air temperature was measured just above the carburetor top deck by six thermocouples connected in parallel. The inlet-manifold mixture temperature in the intake pipes was obtained by averaging the temperatures measured by unshielded thermocouples in the intake pipes of cylinders 5, 9, 13, and 17. One thermocouple was located in each of the four intake pipes approximately 6 inches from the intake port.

All of the thermocouples with the exception of those indicating the exhaust-gas temperature were iron-constantan thermocouples; all temperatures were read on a self-balancing potentiometer.

PROCEDURE

The engine speed, the inlet-manifold pressure, and the fuel-air ratio were maintained at the desired values for each run while the exhaust pressure was varied in increments from approximately 7 inches of mercury absolute to about 20 inches of mercury above the inlet-manifold pressure. Most of the runs were made with the supercharger in low gear ratio; however, runs at three engine speeds (1200, 1800, and 2400 rpm), one inlet-manifold pressure (34 in. Hg absolute), and one fuel-air ratio (0.085) were repeated with the supercharger in high gear ratio. The nominal engine-operating conditions at which the runs were made are presented in table I.

All data were obtained with the engine throttle full open. In order to keep the inlet-manifold pressure constant, at most conditions the carburetor-inlet pressure had to be slightly decreased as the exhaust pressure was increased. The maximum change was about 0.6 inch of mercury for the range of exhaust pressures covered, although in most cases it was much less. At low engine speeds and with the supercharger in low gear ratio it was sometimes necessary to use the laboratory combustion-air supply in order to obtain the high inlet-manifold pressures.

For each series of runs with variable exhaust pressure, the cooling-air pressure drop was set at such a value that the maximum rear spark-plug-gasket temperature was between 375° and 425° F when

the exhaust pressure was approximately 28 inches of mercury absolute. The cooling-air pressure drop was maintained at this value while the exhaust pressure was varied over the desired range. Sufficient time was allowed at each exhaust pressure for the cylinder temperatures to reach equilibrium. The oil-in temperature was maintained at $160^{\circ} \pm 5^{\circ}$ F.

METHODS OF CALCULATION

Effect of exhaust pressure on indicated power. - In reference 2 it is shown that, for a given engine, engine speed, inlet-manifold mixture temperature, and fuel-air ratio, the effect of exhaust pressure on engine indicated power can be represented by plotting the dimensionless ratio ϕ of the indicated mean effective pressure to the inlet-manifold pressure against the ratio of exhaust pressure to inlet-manifold pressure. The resulting curves are shown to be approximately independent of inlet-manifold pressure. Thus

$$\phi = \frac{\text{imep}}{P_m} = F \left(\frac{p_e}{P_m}, N, T_m, f \right) \quad (1)$$

where

imep indicated mean effective pressure, (lb/sq ft)

P_m inlet-manifold pressure, (lb/sq ft absolute)

p_e exhaust pressure, (lb/sq ft absolute)

N engine speed, (rpm)

T_m inlet-manifold mixture temperature, ($^{\circ}$ R)

f fuel-air ratio

For any given run with variable exhaust pressure, the engine speed and the fuel-air ratio were held constant. Because facilities were unavailable for varying the carburetor-air temperature, the inlet-manifold mixture temperature could not be held constant. The indicated horsepower (and hence ϕ) was corrected to a constant inlet-manifold mixture temperature of 660° R on the assumption that it varied inversely as the absolute inlet-manifold mixture temperature. For engines having variable spark timing, the spark advance would have an appreciable effect on ϕ for otherwise constant operating conditions.

Additional variables exist that also influence ϕ but, for a given engine, their effect is generally small as compared with the variables listed in equation (1).

The quantity ϕ was computed from the experimental data by

$$\phi = \frac{\text{imep}}{p_m} = \frac{2 \times 33,000 \text{ ihp}}{p_m v_d N}$$

where v_d is the displacement volume of the engine in cubic feet. The indicated horsepower is defined by

ihp = brake horsepower + supercharger horsepower + friction horsepower

and this is seen to include the contributions of all four strokes of the cycle. The brake horsepower was obtained from the dynamometer tests.

Supercharger power was obtained by

$$\text{shp} = \frac{q}{\eta} \frac{W_c (1 + f) U^2}{550 g \eta_g}$$

where

W_c measured charge-air flow, (lb/sec)

U supercharger impeller tip speed, (ft/sec)

g acceleration due to gravity, (ft/sec²)

η_g supercharger-drive-gear efficiency, assumed to be 0.85

$\frac{q}{\eta}$ ratio of pressure coefficient to adiabatic efficiency, assumed to be 1.0

The mechanical-friction horsepower was computed from

$$\text{fhp} = K N^2$$

where K is the constant, 3.214×10^{-5} . The value of K corresponding to the bore, the stroke, and the number of cylinders of the engine was determined from an empirical equation based on a large amount of test data obtained on various types of reciprocating engine. The friction horsepower thus determined is due only to rubbing and excludes pumping power.

Effect of exhaust pressure on brake power. - In addition to presenting the variation of brake power with exhaust pressure, the ratio α of brake power at any value of p_e/p_m to the value at $p_e/p_m = 1.0$ for the same engine speed, inlet-manifold pressure, carburetor-air temperature, and fuel-air ratio is plotted against p_e/p_m . The brake horsepower at $p_e/p_m = 1.0$ was determined from faired curves of corrected brake horsepower. The brake power was corrected to a carburetor-air temperature of 550°R on the conventional assumption that it varied inversely as the square root of the absolute carburetor-air temperature. This correction was quite small because the carburetor-air temperature varied no more than $\pm 15^\circ \text{F}$ from 90°F for most cases during the investigation.

Effect of exhaust pressure on volumetric efficiency. - Volumetric efficiency η_v was computed by the relation

$$\eta_v = \frac{120 R T_m W_c}{p_m v_d N} \quad (2)$$

where

R gas constant for air, (ft-lb)/(lb)(°F)

Variation of power with charge-air flow. - For a given engine, spark setting, and fuel-air ratio, the power defined by the contribution of the compression and expansion strokes is approximately proportional to the charge air in the cylinder at the instant of valve closure. An estimate of this power was obtained by subtracting the pumping horsepower php from the indicated horsepower ihp . The pumping power was based on a square indicator card and was calculated by

$$php = (p_m - p_e) \frac{v_d N}{2 \times 33,000}$$

RESULTS AND DISCUSSION

Effect of Exhaust Pressure on Indicated Power

The variation of ϕ with p_e/p_m is shown in figure 3 for several constant engine speeds and three fuel-air ratios. The curves, which are independent of inlet-manifold pressure for the range of manifold pressures covered, show that for any given inlet-manifold pressure the indicated power increases at a diminishing rate as the exhaust pressure decreases.

The correction for inlet-manifold mixture temperature seems to be justified by the fact that the data obtained with the supercharger in high gear ratio agree fairly well with the low-gear data. (See curves for 1800 and 2400 rpm, fig. 3(b).) Inasmuch as the data for the high-gear-ratio operation were obtained with approximately the same carburetor-air temperature as the low-gear data, for the same engine speed an appreciable difference in inlet-manifold mixture temperature existed. The standard mixture temperature of 660° R was arbitrarily chosen; but, if the manner in which indicated power varies with mixture temperature is known, the data can be corrected to any desired mixture temperature without affecting the correlation.

In the present investigation, with a constant carburetor-air temperature T_c , the inlet-manifold mixture temperature T_m slightly increased with an increase in exhaust pressure. The quantity $T_m - T_c$ plotted against p_e/p_m is shown in figure 4 for all engine speeds, inlet-manifold pressures, and fuel-air ratios. Although the variation of mixture temperature with exhaust pressure is seen to be small for this engine, the effect is probably more pronounced on engines having a valve overlap larger than that of this engine.

Effect of Exhaust Pressure on Brake Power

Variation of brake horsepower and α with p_e/p_m . - The brake horsepower, corrected to a carburetor-air temperature of 550° R and with the supercharger in low gear ratio, is plotted against p_e/p_m in figure 5 for various engine speeds and inlet-manifold pressures and for three fuel-air ratios. The values of brake horsepower with the supercharger in high gear ratio at engine speeds of 1200, 1800, and 2400 rpm are shown in figure 6 for a fuel-air ratio of 0.085 and a constant inlet-manifold pressure of 34 inches of mercury absolute. From the faired curves in figures 5 and 6, the brake horsepowers at $p_e/p_m = 1.0$ were determined.

The quantity α (ratio of brake horsepower at any value of p_e/p_m to that at $p_e/p_m = 1.0$ for the same altitude, engine speed, inlet-manifold pressure, carburetor-air temperature, and fuel-air ratio) is used as a measure of the effect of exhaust pressure on engine brake horsepower. Figure 7(a) shows this ratio α as obtained from figure 5(a) plotted against p_e/p_m for constant engine speeds and a fuel-air ratio of 0.100. A single faired curve is obtained for each engine speed regardless of inlet-manifold pressure. Corresponding plots for fuel-air ratios of 0.085 and 0.069 are shown in figures 7(b) and 7(c), respectively. Comparison of the curves of figure 7 shows that

for these tests the ratio α was independent of fuel-air ratio; the same faired curve is therefore used for a given engine speed regardless of the fuel-air ratio.

Brake horsepower and α shown in figures 5 and 7, respectively, are for the supercharger in low gear ratio. In figure 8 the faired curves of α as obtained from figure 7 for engine speeds of 1200, 1800, and 2400 rpm are compared with points of α for the supercharger in high gear ratio. The effect of supercharger-gear ratio on α is small. For operation at high gear ratio, the use of α as given for low gear ratio and the corresponding engine speed would introduce an error of approximately $1\frac{1}{2}$ percent in brake-horsepower prediction for a change in p_e/p_m from 0.2 to 1.0.

In figure 9 a single curve of α plotted against p_e/p_m for each engine speed includes data for all inlet-manifold pressures, three fuel-air ratios, and with the supercharger in both high and low gear ratio. The effect of exhaust pressure on power as defined by α is seen to be greater at the low than at the high engine speeds for values of p_e/p_m less than 1.0. When p_e/p_m is greater than 1.0, the effect of exhaust pressure on α is practically independent of engine speed.

In this investigation the exhaust pressures were often considerably less than the carburetor-inlet pressure; consequently, the brake horsepowers measured under the test conditions were higher than would be obtained if the engine were charged with the power required by a geared blower to supercharge from an altitude pressure to the carburetor-inlet pressure measured under the test conditions. Computations show, however, that the curves of α are unchanged if the engine is charged with the additional supercharger work. For example, if the altitude pressure is 8.88 inches of mercury absolute (30,000 ft) and the carburetor-inlet pressure as measured during the run is 20 inches of mercury absolute, the entire curve of brake horsepower plotted against p_e/p_m would be lowered by the amount of geared-supercharger power required to compress the air from 8.88 to 20 inches of mercury absolute. The charge-air flow is nearly proportional to the engine power with the result that the additional supercharger power under consideration is likewise nearly proportional to the engine power. Thus the values in both the numerator and denominator of α are decreased an amount substantially proportional to the original values and the effect on α of including the additional supercharger power is small. As previously mentioned, the carburetor-inlet pressure decreased as the exhaust pressure was increased with constant inlet-manifold pressure. This effect

would cause a small decrease in supercharger power (about 2 percent for the range of exhaust pressures covered) and one that is negligible in its effect on α .

Example for use of α . - Figure 9 can be used to predict the effect of changes in exhaust pressure on engine brake horsepower at various operating conditions provided that the operating conditions at one point are known. (Operating conditions may be obtained from the manufacturer's calibration.) For example, the following conditions are assumed:

Engine speed, rpm	2400
Inlet-manifold pressure, inches of mercury absolute	29
Exhaust pressure, inches of mercury absolute	17
Brake horsepower	1150

The following relation is used to determine the brake horsepower when the exhaust pressure is increased to 35 inches of mercury absolute with no change in altitude:

$$\text{bhp}_2 = \text{bhp}_1 \frac{\alpha_2}{\alpha_1}$$

where

bhp_1 known value of bhp

bhp_2 desired value of bhp

α_1 ratio determined from figure 9 for specified engine speed and $P_e/P_m = 17/29 = 0.59$

α_2 ratio determined from figure 9 for same engine speed and $P_e/P_m = 35/29 = 1.21$

From figure 9, α_1 is found to be 1.09 and α_2 is found to be 0.937; therefore, the brake horsepower at the new exhaust pressure is

$$\text{bhp}_2 = .1150 \frac{0.937}{1.09} = 989$$

If the change in exhaust pressure in this example is caused by a change in altitude, then corrections must also be applied for any changes in supercharger work and carburetor-air temperature.

Effect of Engine Speed on p_m/p_c

The brake horsepower was measured with the engine throttle in the full-open position and the carburetor was supplied with air from the laboratory air system at a pressure sufficient to give the desired pressure at the inlet manifold. The variation of the ratio of inlet-manifold pressure to full-throttle carburetor-inlet pressure p_m/p_c with engine speed N is shown in figure 10. This faired curve, which is for a carburetor-air temperature of $550^\circ R$, is included to facilitate the determination of p_c for the various operating conditions and in combination with the values of charge-air flow may be used to compute the auxiliary-supercharger power for any altitude. The curve is accurate to ± 1.0 percent for values of p_e/p_m near 1.0 and to about ± 2.0 percent over the range of p_e/p_m covered.

Effect of Exhaust Pressure on Charge-Air

Flow and Volumetric Efficiency

The variation of charge-air flow W_c , corrected to a carburetor-air temperature of $550^\circ R$, with p_e/p_m for constant inlet-manifold pressures is shown in figure 11 for operation with the supercharger in low gear ratio. At all conditions the charge-air flow decreased as exhaust pressure increased. At high inlet-manifold pressures, low exhaust pressures, and low engine speeds, the air flow tended to increase sharply as the exhaust pressure decreased. The effect could possibly be due to the high value of $p_m - p_e$, which tends to open the intake valve early. Curves for operation with the supercharger in high gear ratio and for an inlet-manifold pressure of 34 inches of mercury absolute are shown in figure 12.

Volumetric efficiency η_v is plotted in figure 13 against p_e/p_m for constant engine speeds, various inlet-manifold pressures, and three fuel-air ratios. The values for high-gear-ratio operation are included in figure 13(b) and are seen to agree with the data for low gear ratio at the same inlet-manifold pressure and engine speed. For all conditions the volumetric efficiency decreases as the exhaust pressure increases.

All the data of figure 13 are shown in figure 14 with the various fuel-air ratios plotted on a single curve for any given inlet-manifold pressure and engine speed. For a given engine speed and inlet-manifold

pressure, volumetric efficiency is seen to be practically independent of fuel-air ratio. The volumetric efficiency is also independent of inlet-manifold pressure for a given speed except at points where blow-through occurs.

Volumetric efficiency was calculated by equation (2) using the charge-air flow, the measured inlet-manifold mixture temperature, and the gas constant for air. A progressive increase in mixture temperature was found to exist from the blower rim to the engine intake ports; the temperature rise was of the order of 60° F. The most logical temperature on which to base a volumetric efficiency would be the one nearest the cylinder; however, as the unshielded thermocouples in the intake ports would be considerably influenced by radiation from the cylinder, the temperatures in the intake pipes about 6 inches upstream of the intake ports were used. These temperatures, of course, are subject to any inaccuracy caused by incomplete vaporization of the fuel.

The total charge flow (fuel plus air) and the gas constant for the mixture of fuel and air might seem more correct to use in the calculation of volumetric efficiency η_v (equation (2)); however, the quantity $R_m(1+f)$, where R_m is the gas constant of the mixture, does not vary appreciably with fuel-air ratio and thus the corresponding values of η_v given by equation (2) are also nearly independent of fuel-air ratio for the range covered by this investigation. The quantity $R_m(1+f)$ is several percent larger than the value of R for air and the corresponding volumetric efficiencies would be increased accordingly by an approximately constant factor. The trends obtained with the two volumetric efficiencies would thus remain approximately the same.

Variation of Power with Charge-Air Flow

The difference between indicated horsepower and pumping horsepower ($i\text{hp} - \text{php}$) is plotted against charge-air flow W_c in figure 15. This difference represents the work of only the compression and expansion strokes of the cycle. Separate plots are shown for each fuel-air ratio and each plot is keyed according to engine speed. The data obtained over the range of exhaust pressures at each inlet-manifold pressure are included in the points shown for each engine speed. All the data shown are for the supercharger in low gear ratio. The power and charge-air-flow curves were corrected to a constant inlet-manifold mixture temperature of 660° R. The few data points in figure 15 that show a relatively large deviation from the curve correspond to operation at low values of p_c/p_m , low engine speeds,

and high inlet-manifold pressures where appreciable blow-through of the charge air probably occurs, as indicated by figures 11 to 14. The correlation is affected to some extent by the assumptions made in determining indicated horsepower and pumping horsepower and possibly to changes in thermal efficiency.

Effect of Exhaust Pressure on Cylinder-Head Temperatures

In order to show briefly how cylinder-head temperatures vary with exhaust pressure, the quantity $(T_h - T_a)/(T_h - T_a)_1$ is plotted against p_e/p_m for constant engine speeds, fuel-air ratios, and cooling-air pressure drops in figure 16. The quantity $(T_h - T_a)$ is the difference between average cylinder-head temperature and inlet cooling-air temperature; $(T_h - T_a)_1$ is the corresponding value at $p_e/p_m = 1.0$ for the same engine speed, inlet-manifold pressure, fuel-air ratio, and cooling-air pressure drop. The cylinder-head temperature is taken as the average of the temperature indications of the thermocouples deeply embedded in the rear-spark-plug bosses. The cooling-air pressure drops across the cylinder heads remained nearly constant for each set of runs at variable exhaust pressure. The maximum and minimum values are given in figure 16. The pressure drop, however, did vary for the various speeds, inlet-manifold pressures, and fuel-air ratios. The ratio $(T_h - T_a)/(T_h - T_a)_1$ is seen to increase as p_e/p_m increased. The effect of exhaust pressure on cylinder temperature increases as the fuel-air ratio is decreased over the range investigated.

Effect of Exhaust Pressure on Exhaust-Gas Temperature

The exhaust-gas temperatures obtained by averaging the readings of the three thermocouples in the exhaust collector are plotted against p_e/p_m in figure 17 for the various engine operating conditions. The readings obtained from the three thermocouples for any one datum point were within a temperature range of 30° F. The temperatures increased with engine speed and inlet-manifold pressure and as the fuel-air ratio decreased from 0.100 to 0.069.

An attempt was made to seal the exhaust system ahead of the thermocouples in order that air could not leak into the collector and cause afterburning when the exhaust pressure was below atmospheric. In some cases where leaks did develop during a running period, the temperature rapidly increased 100° to 200° F. These values are not shown in figure 17.

The exhaust-gas temperatures as measured in this investigation will probably not apply with great accuracy for turbine computations in flight installations where the exhaust system is shrouded and cooled or where large amounts of ducting exist between the engine and the nozzle box.

A few runs were made with the exhaust collector insulated with 1 to $1\frac{1}{2}$ inches of insulating cement. The collector was insulated from the plane of the rear-row exhaust ports to about 1 foot beyond the point at which the thermocouples were located. The temperatures were about 250° F higher than those obtained with the uninsulated collector. Several failures in the exhaust collector occurred owing to the abnormally high temperatures to which it was subjected and only a small amount of data was taken.

SUMMARY OF RESULTS

The following results were obtained from an investigation to determine the effect of exhaust pressure on engine performance on an 18-cylinder, air-cooled radial engine operated at engine speeds from 1200 to 2400 rpm, inlet-manifold pressures from 30 to 45 inches of mercury absolute, fuel-air ratios of 0.069, 0.085, and 0.100, and exhaust pressures from approximately 7 inches of mercury absolute to about 20 inches of mercury above inlet-manifold pressure:

1. For constant values of engine speed, inlet-manifold pressure, and fuel-air ratio, the engine power increased at a diminishing rate as exhaust pressure decreased.

2. For any given engine speed and fuel-air ratio, good correlation of the power data over the complete range of inlet-manifold pressure and exhaust pressure was obtained by plotting the ratio of indicated mean effective pressure to inlet-manifold pressure against the ratio of exhaust pressure to inlet-manifold pressure.

3. When α (the ratio of the brake horsepower at any exhaust pressure to the brake horsepower at the same engine speed, fuel-air ratio, and inlet-manifold pressure but at an exhaust pressure equal to the inlet-manifold pressure) was plotted against the ratio of exhaust pressure to inlet-manifold pressure, a single curve resulted regardless of inlet-manifold pressure, exhaust pressure, or fuel-air ratio. The shape of the curve of α plotted against the ratio of exhaust pressure to inlet-manifold pressure varied with engine speed.

4. At constant conditions of fuel-air ratio, engine speed, inlet-manifold pressure, and cooling-air pressure drop, the average cylinder-head temperatures increased as the exhaust pressure increased. The effect became more marked as the fuel-air ratio decreased from 0.100 to 0.069.

Aircraft Engine Research Laboratory,
National Advisory Committee for Aeronautics,
Cleveland, Ohio, December 3, 1946.

REFERENCES

1. Hannum, Richard W., and Zimmerman, Richard H.: Calculations of the Economy of an 18-Cylinder Radial Aircraft Engine with an Exhaust-Gas Turbine Geared to the Crankshaft at Cruising Speed. NACA ARR No. E5K28, 1945.
2. Pinkel, Benjamin: Effect of Exhaust Back Pressure on Engine Power. NACA CB No. 3F17, 1943.
3. Valerino, Michael F., Kaufman, Samuel J., and Hughes, Richard F.: Effect of Exhaust Pressure on the Cooling Characteristics of an Air-Cooled Engine. NACA TN No. 1221, 1947.
4. Moore, Charles S., Biermann, Arnold E., and Voss, Fred: The NACA Balanced-Diaphragm Dynamometer-Torque Indicator. NACA RB No. 4C28, 1944.

TABLE I - OPERATING CONDITIONS

Nominal engine speed (rpm)	Nominal fuel-air ratio	Nominal inlet-manifold pressure (in. Hg absolute)	Super-charger-gear ratio	Nominal engine speed (rpm)	Nominal fuel-air ratio	Nominal inlet-manifold pressure (in. Hg absolute)	Super-charger-gear ratio			
1200	0.069	30	7.6:1	2000	0.100	34	7.6:1			
1400				2200						
1600				2400						
1800				1400				0.069	40	7.6:1
2000				1600						
1400	0.085	30	7.6:1	1800	0.085	40	7.6:1			
1600				2000						
1800				2200						
2000				2400						
2200				2000				0.100	40	7.6:1
2400	2200									
2000	0.100	30	7.6:1	1800	0.100	40	7.6:1			
2200				2000						
2400				2200						
1400	0.069	34	7.6:1	2400	0.085	45	7.6:1			
1600				1800						
1800				2000						
2000				2200						
1400	0.085	34	7.6:1	1800	0.100	45	7.6:1			
1600				2000						
1800				2200						
2000				2400						
2200				1200				0.085	34	9.45:1
2400	1800									
	2400									

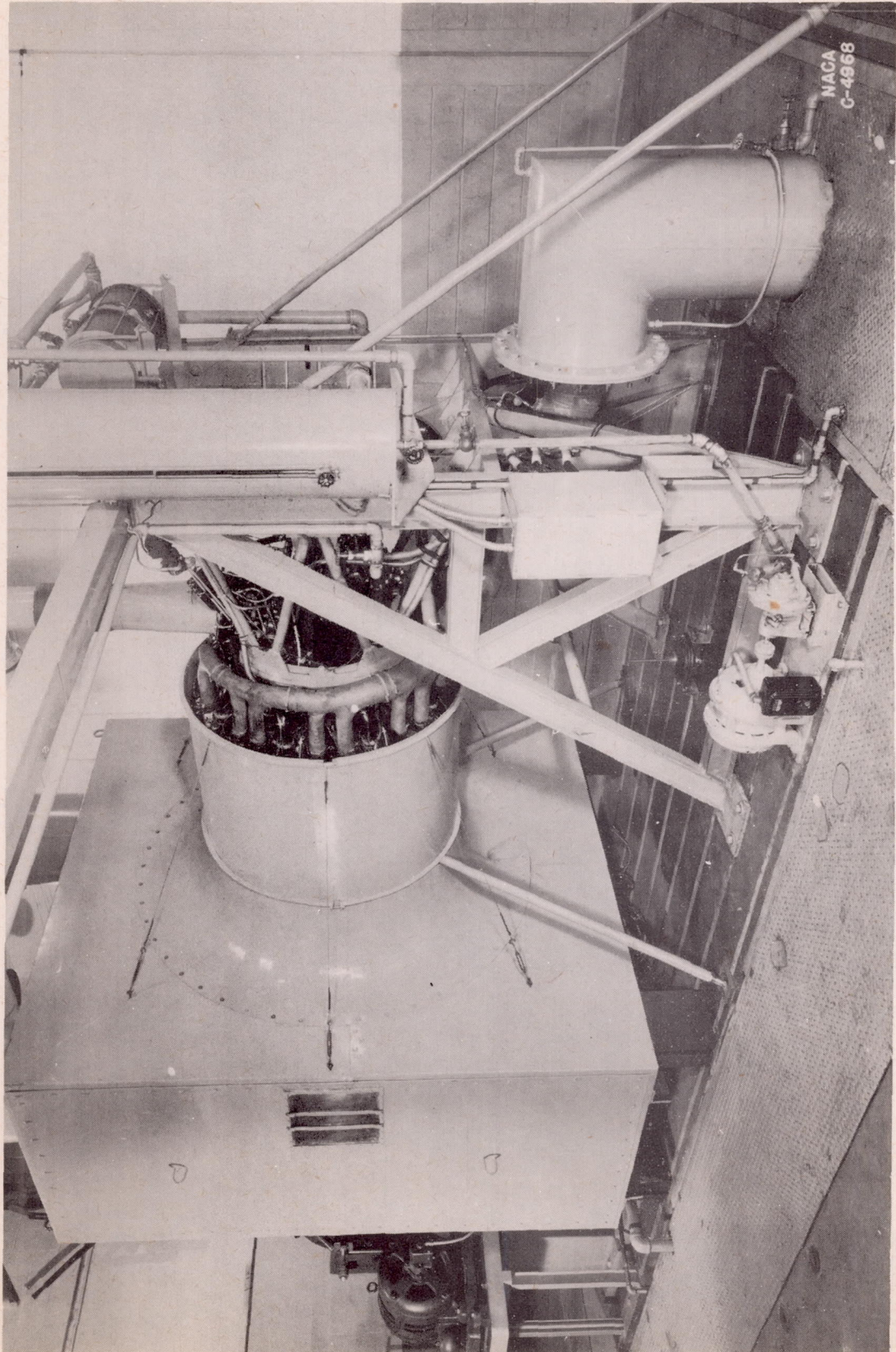
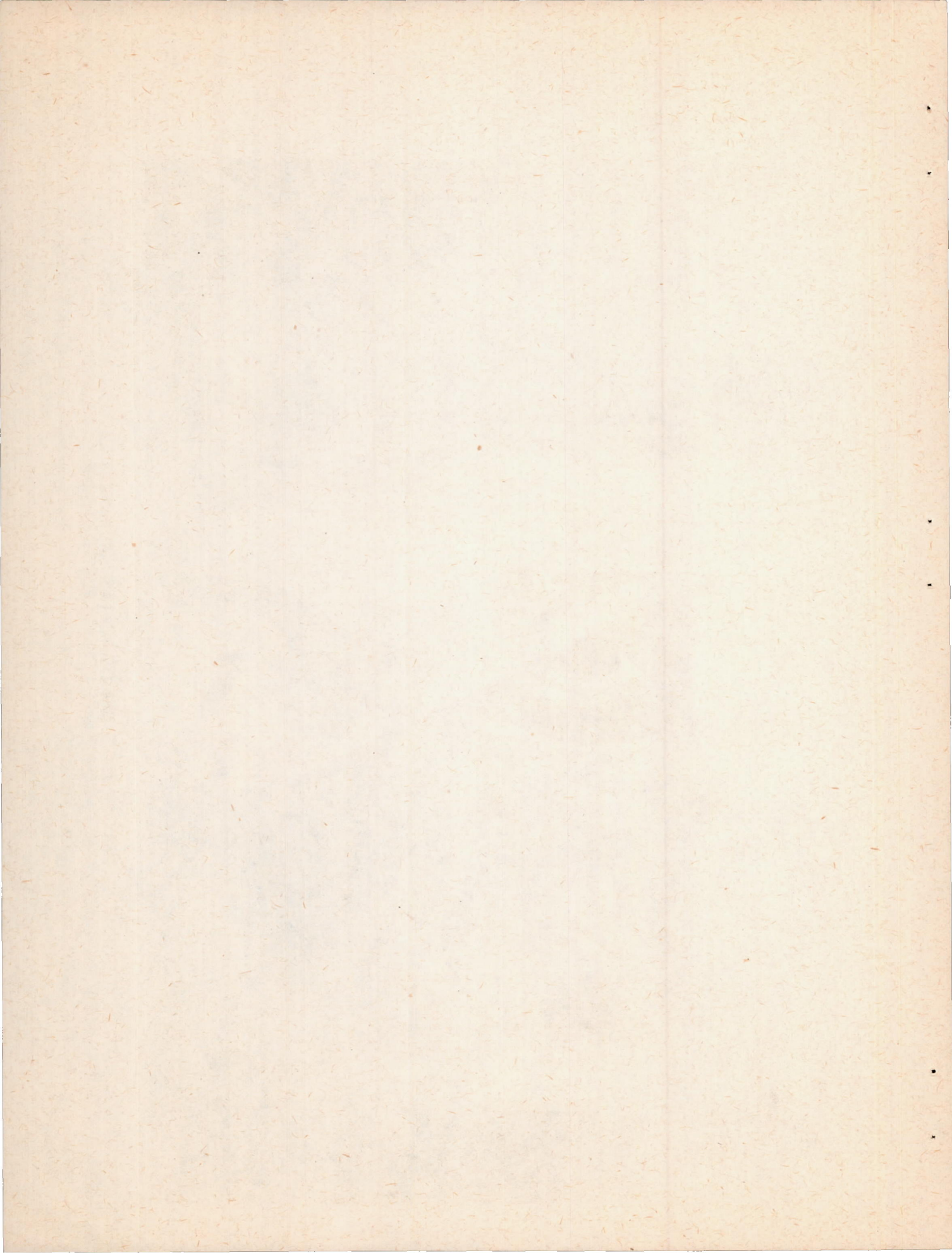
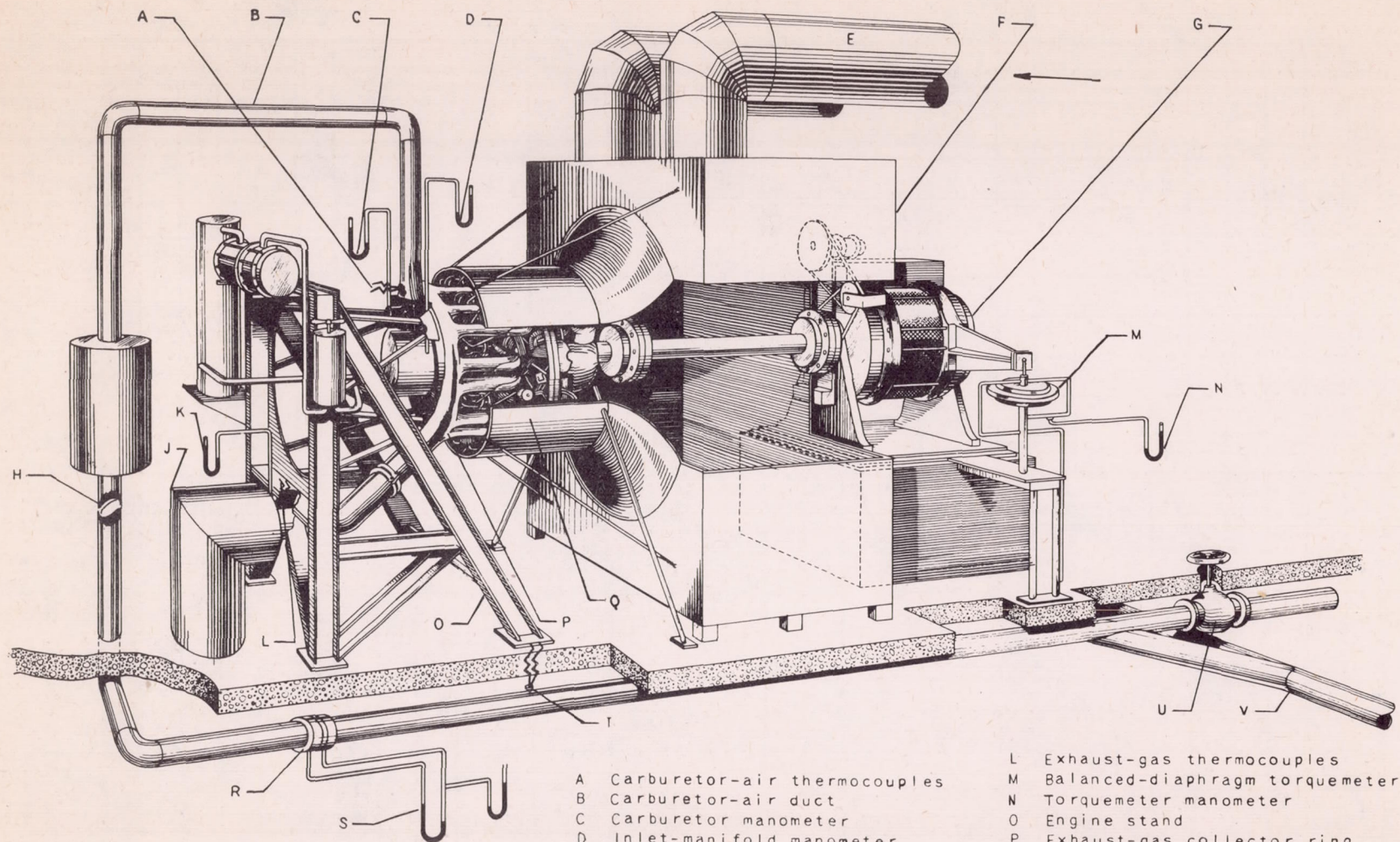


Figure 1. - General view of setup.

690

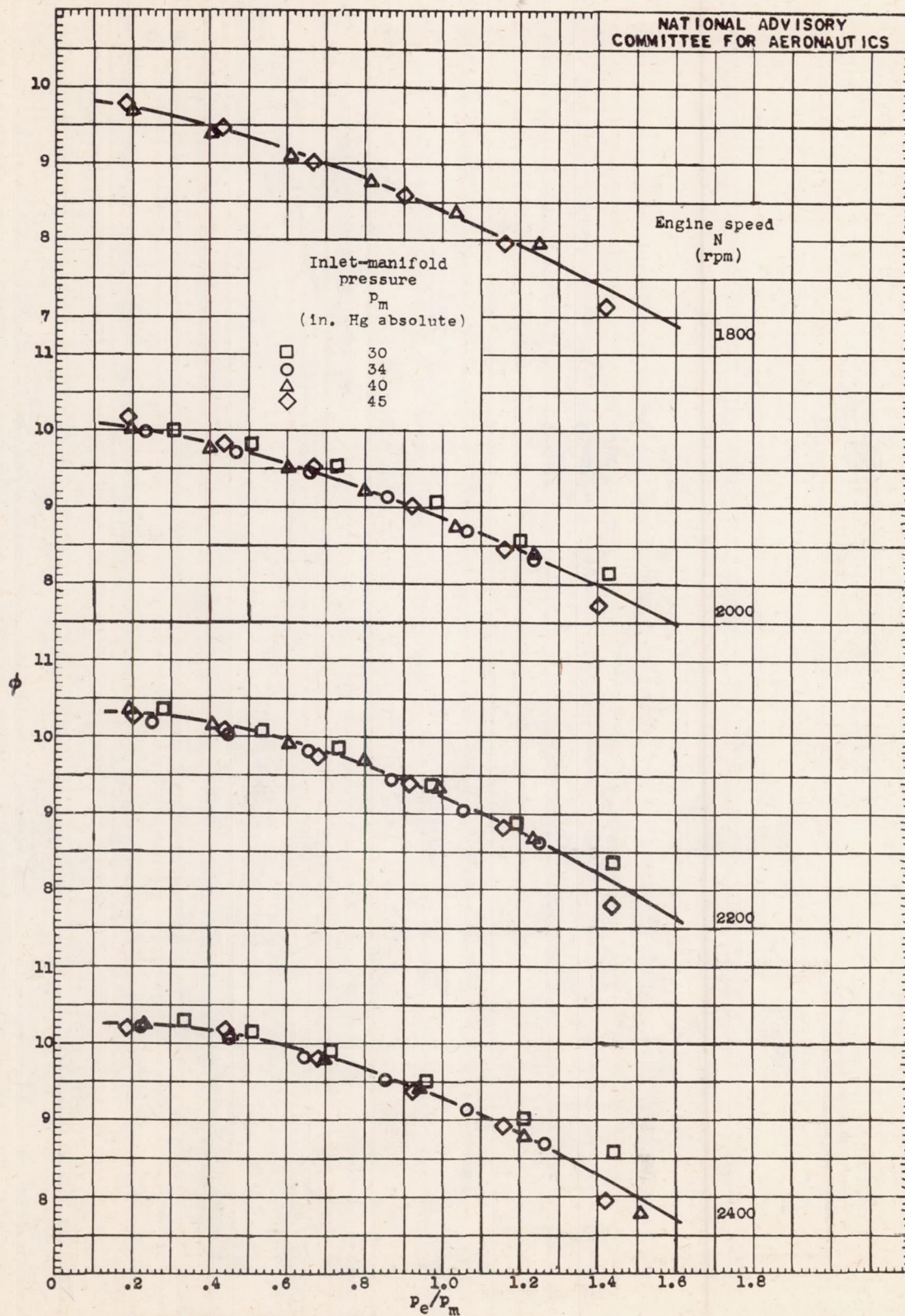




NATIONAL ADVISORY
COMMITTEE FOR AERONAUTICS

- | | | | |
|---|----------------------------------|---|---------------------------------|
| A | Carburetor-air thermocouples | L | Exhaust-gas thermocouples |
| B | Carburetor-air duct | M | Balanced-diaphragm torquemeter |
| C | Carburetor manometer | N | Torquemeter manometer |
| D | Inlet-manifold manometer | O | Engine stand |
| E | Cooling-air pipe | P | Exhaust-gas collector ring |
| F | Cooling-air box | Q | Engine cowling |
| G | Dynamometer | R | Charge-air orifice |
| H | Charge-air butterfly valve | S | Charge-air-orifice manometer |
| J | Elbow section of exhaust ducting | T | Charge-air-orifice thermocouple |
| K | Exhaust manometer | U | Charge-air bleed valve |
| | | V | Combustion-air supply pipe |

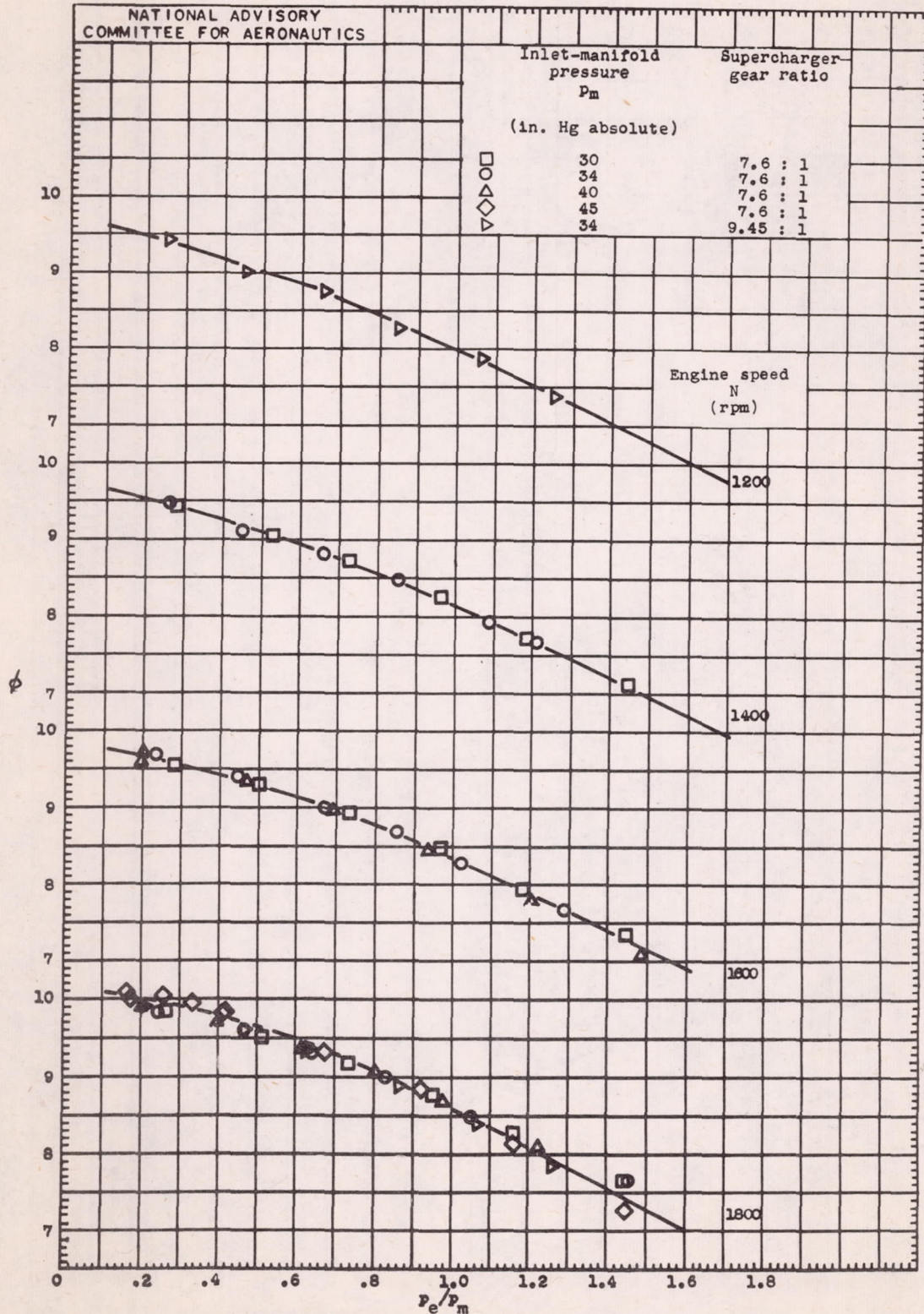
Figure 2. - Sketch of setup.



(a) Fuel-air ratio, 0.100.

Figure 3. - Variation of ϕ with P_e/P_m . Values of ϕ corrected to constant inlet-manifold mixture temperature T_m of 660° R; supercharger in low gear ratio (7.6 : 1) except where otherwise noted.

069



(b) Fuel-air ratio, 0.085.

Figure 3. - Continued. Variation of ϕ with P_e/P_m . Values of ϕ corrected to constant inlet-manifold mixture temperature T_m of $660^\circ R$; supercharger in low gear ratio (7.6 : 1) except where otherwise noted.

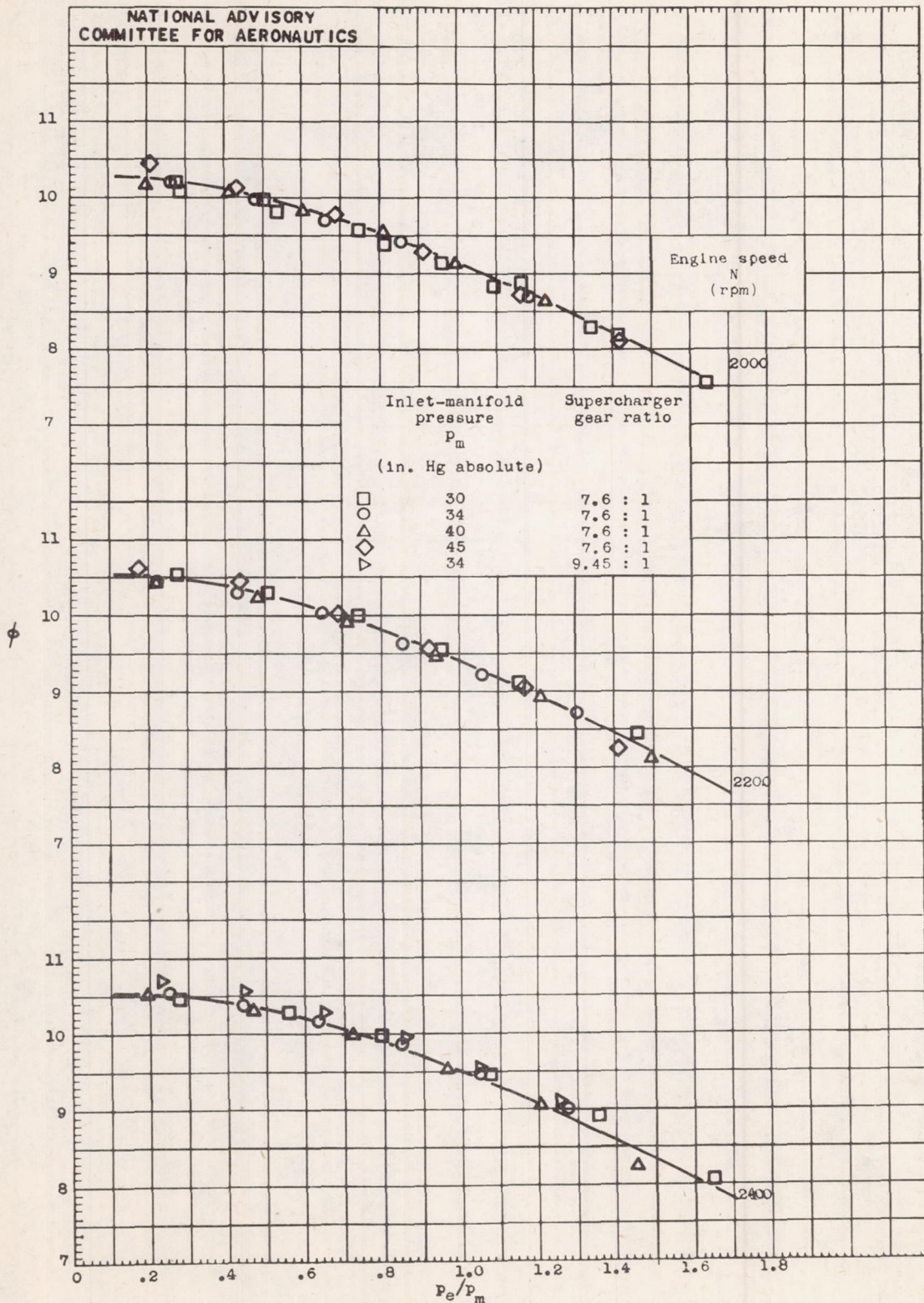
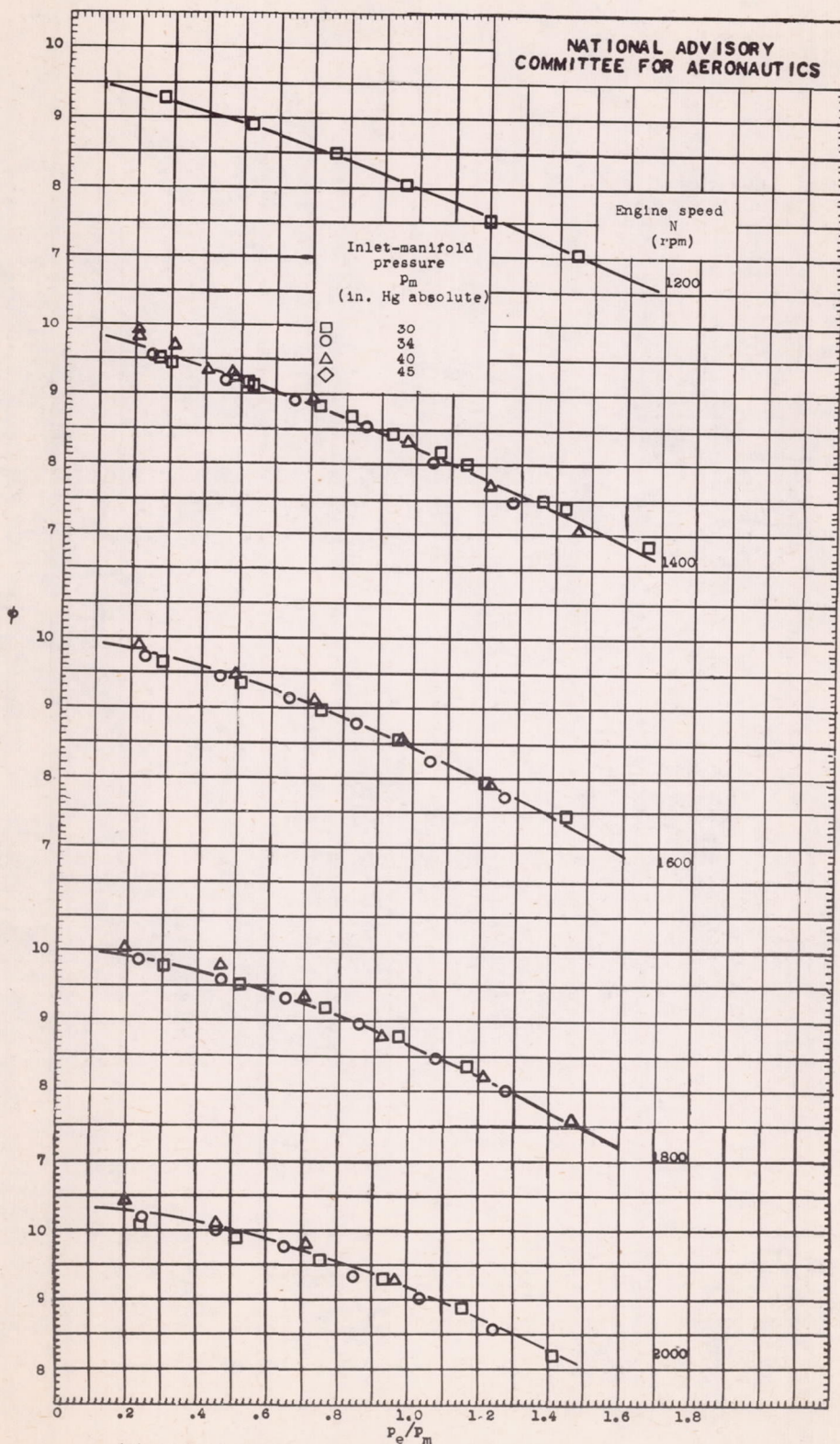


Figure 3. - Continued. Variation of ϕ with p_e/p_m . Values of ϕ corrected to constant inlet-manifold mixture temperature T_m of $660^\circ R$; supercharger in low gear ratio (7.6 : 1) except where otherwise noted.



(c) Fuel-air ratio, 0.069.

Figure 3. - Concluded. Variation of ϕ with p_e/p_m . Values of ϕ corrected to constant inlet-manifold mixture temperature T_m of $660^\circ R$; supercharger in low gear ratio (7.6 : 1) except where otherwise noted.

690

NATIONAL ADVISORY
COMMITTEE FOR AERONAUTICS

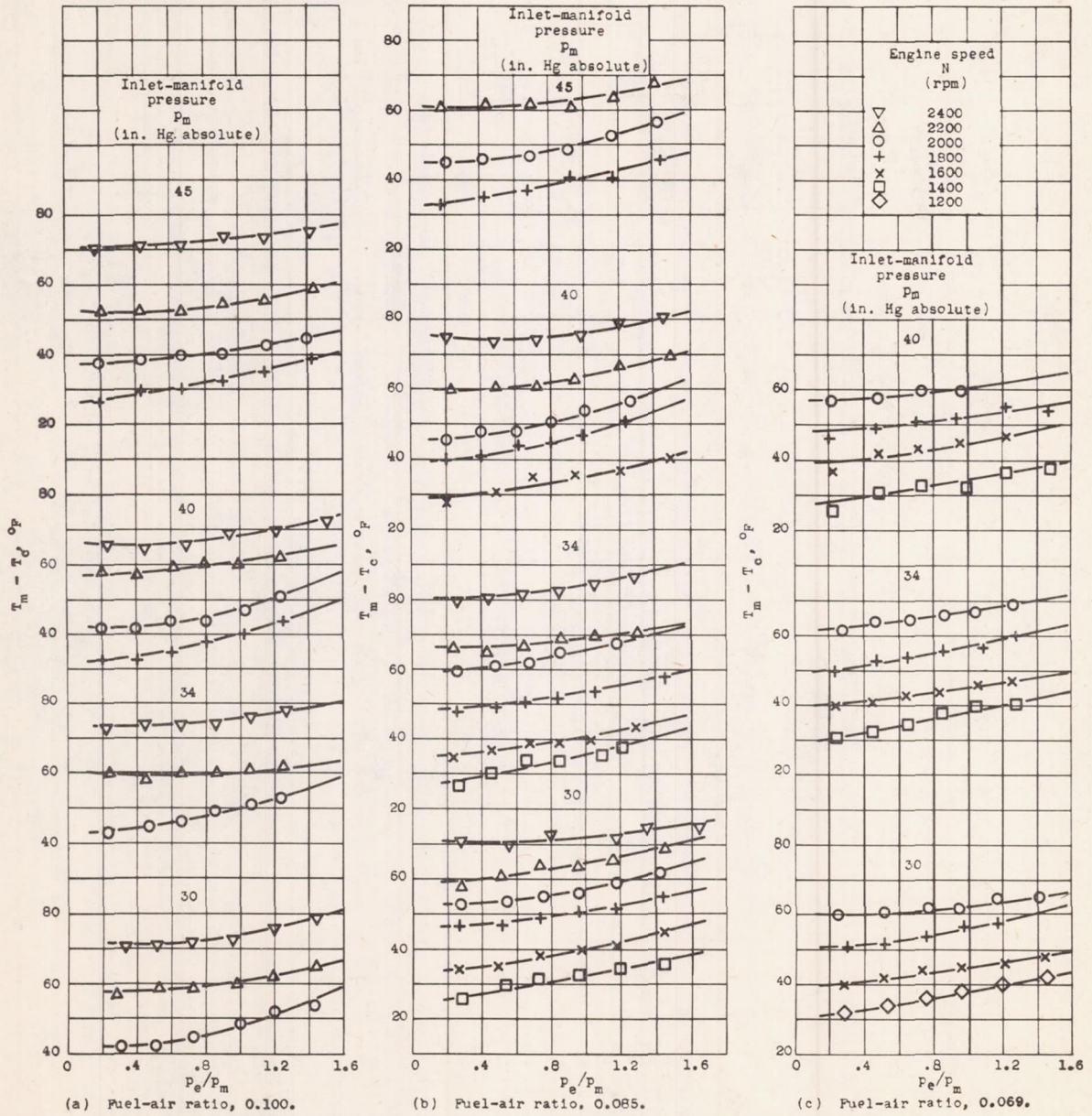
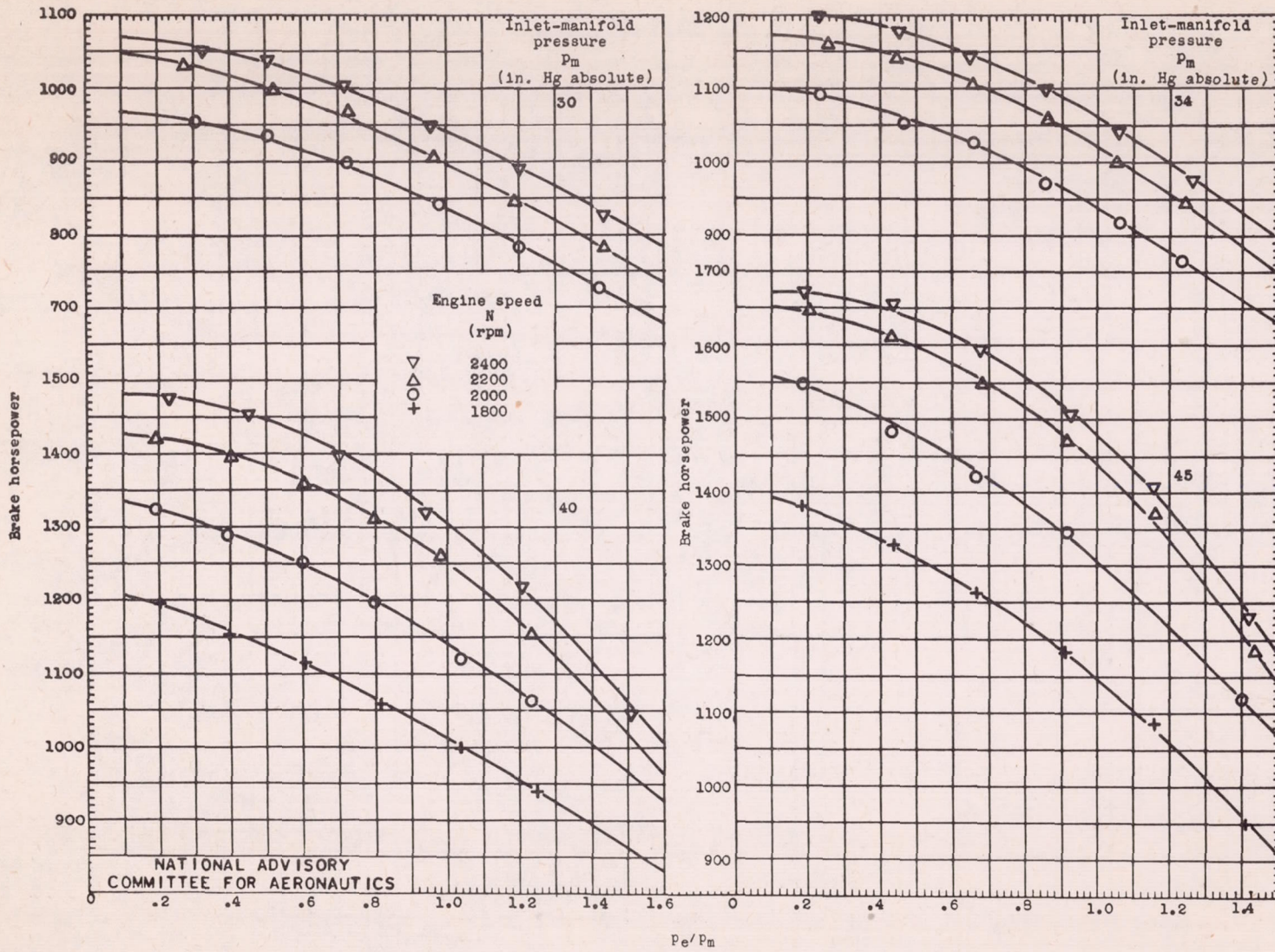


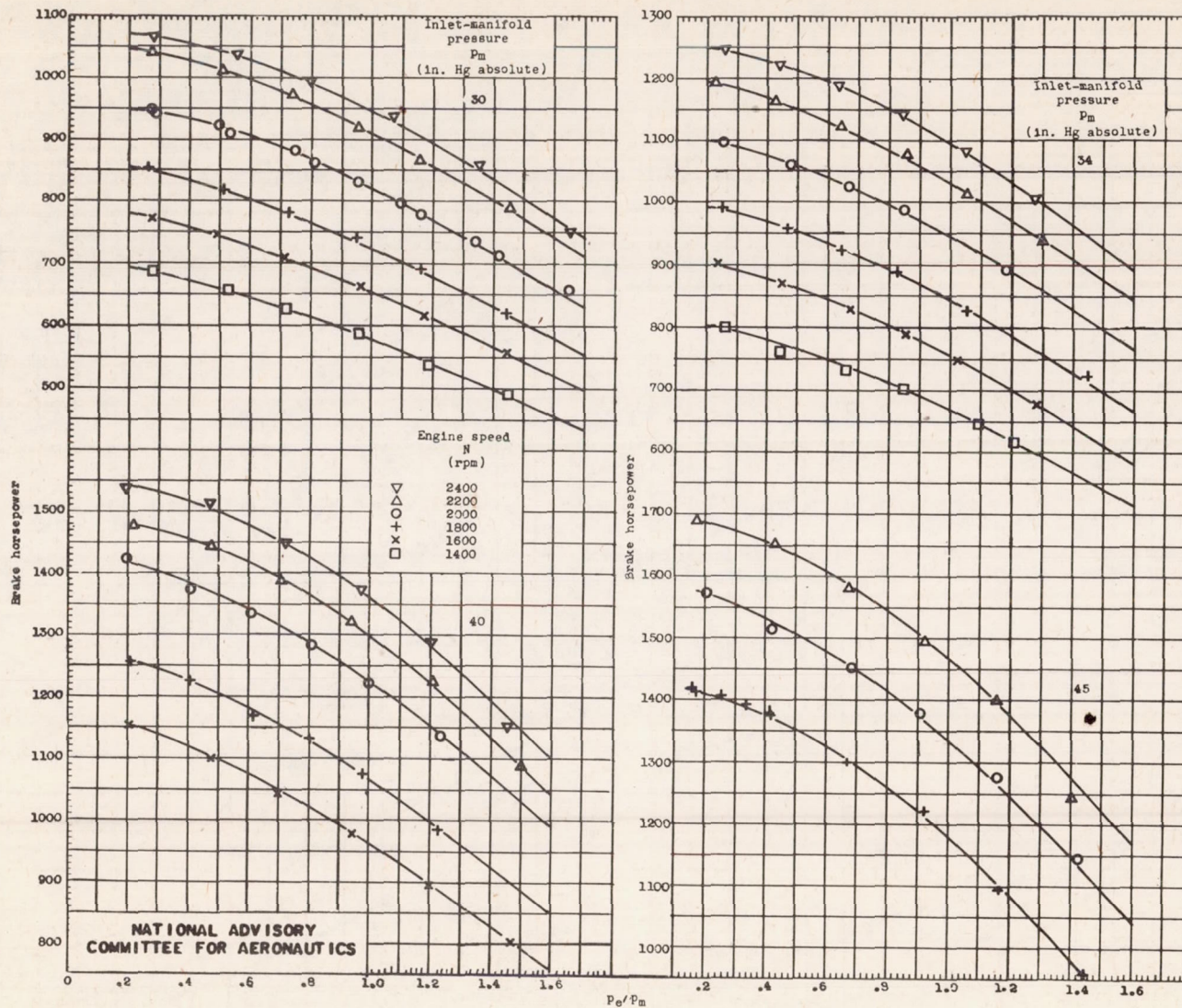
Figure 4.- Variation of $T_m - T_c$ with P_e/P_m with supercharger in low gear ratio (7.6 : 1).

690



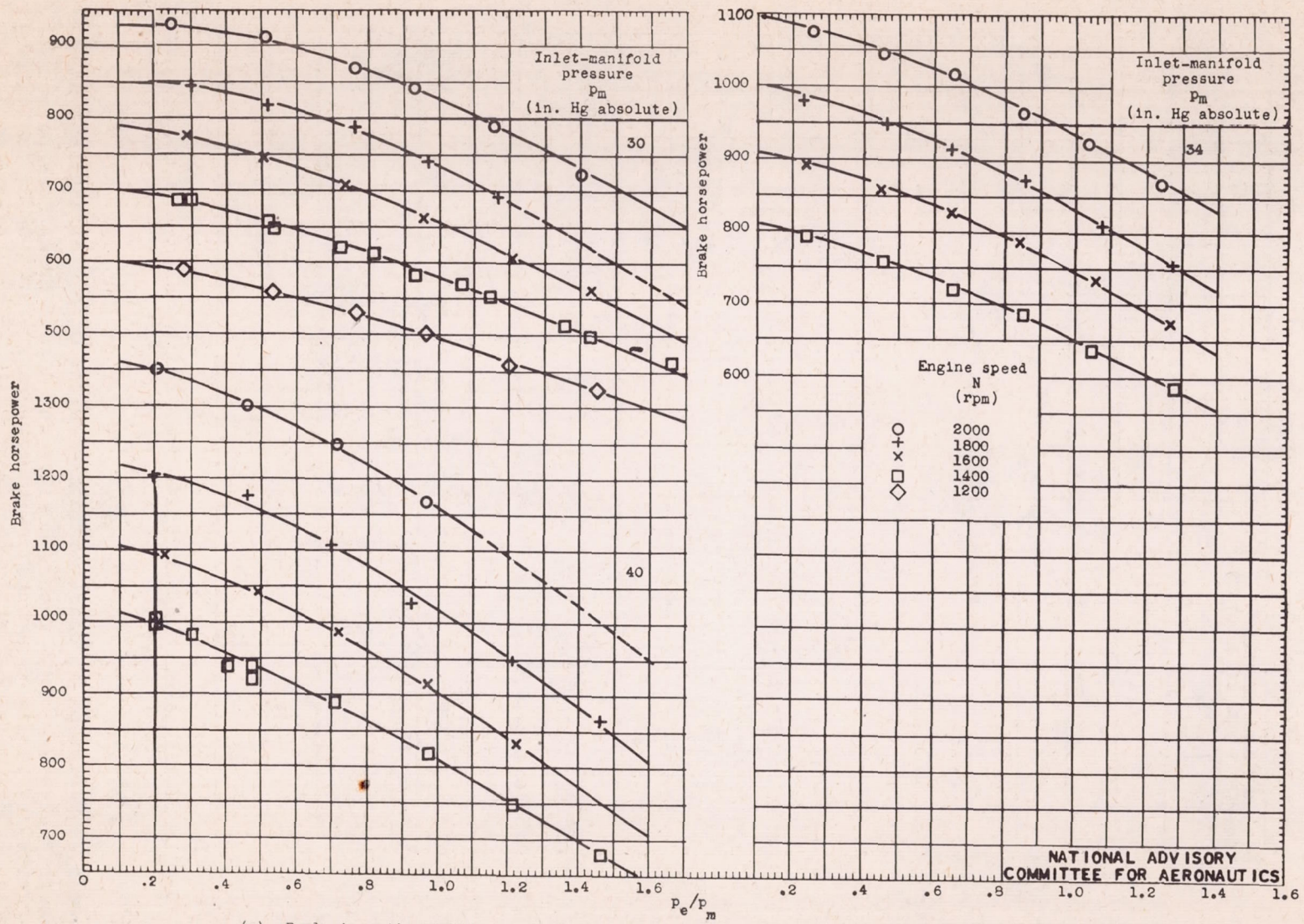
(a) Fuel-air ratio, 0.100.

Figure 5. - Variation of brake horsepower with P_e/P_m . Brake horsepower corrected to constant carburetor-air temperature of 550° R; supercharger in low gear ratio (7.6 : 1).



(b) Fuel-air ratio, 0.095.

Figure 5. - Continued. Variation of brake horsepower with p_0/p_m . Brake horsepower corrected to constant carburetor-air temperature of 550°R ; supercharger in low gear ratio (7.6 : 1).



(c) Fuel-air ratio, 0.089.

Figure 5. - Concluded. Variation of brake horsepower with p_e/p_m . Brake horsepower corrected to constant carburetor-air temperature of 550° R; supercharger in low gear ratio (7.6 : 1).

NATIONAL ADVISORY COMMITTEE FOR AERONAUTICS

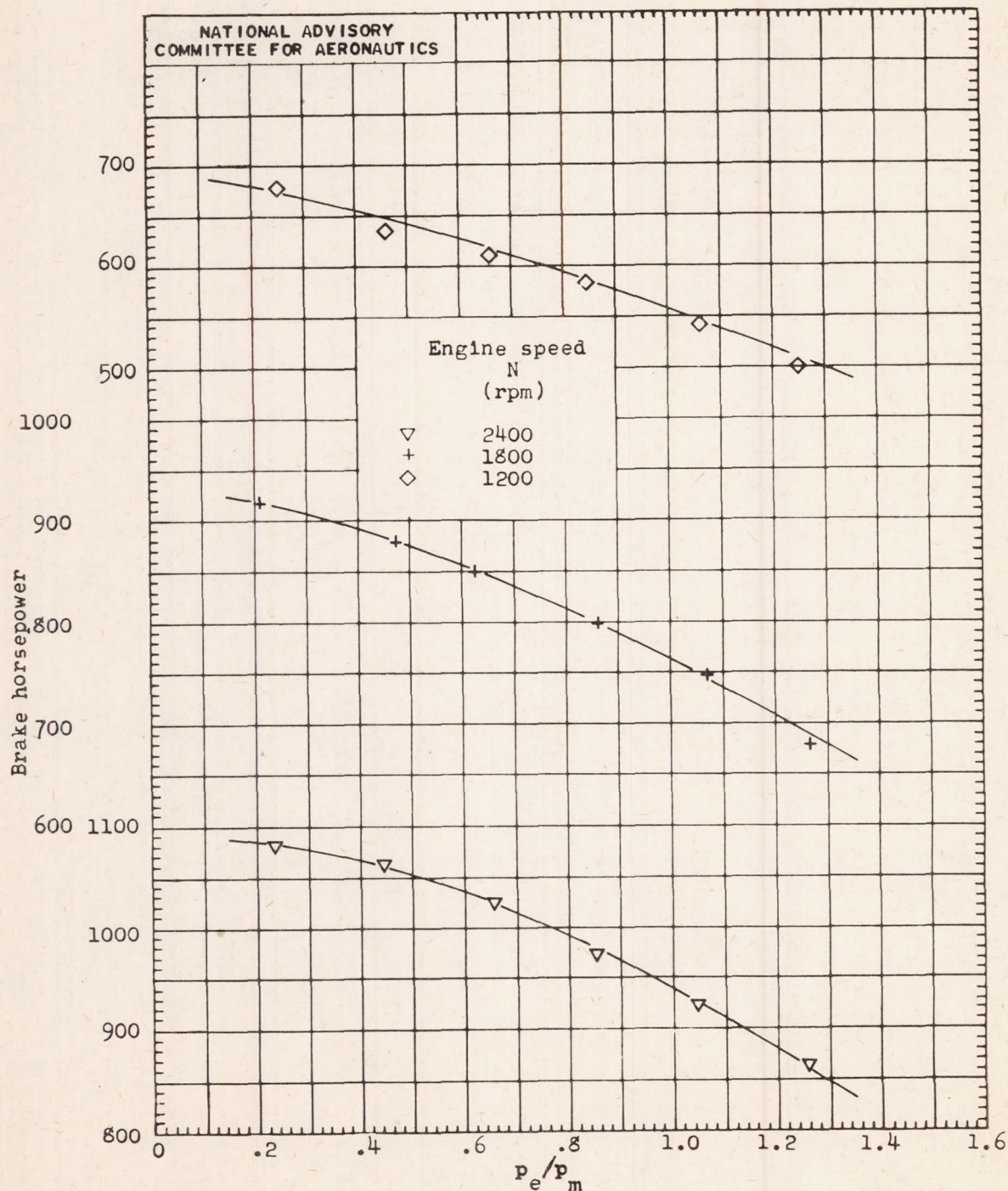


Figure 6. - Variation of brake horsepower with p_e/p_m at constant inlet-manifold pressure of 34 inches mercury absolute. Brake horsepower corrected to constant carburetor-air temperature of 550° R; fuel-air ratio, 0.085; supercharger in high gear ratio (9.45 : 1).

069

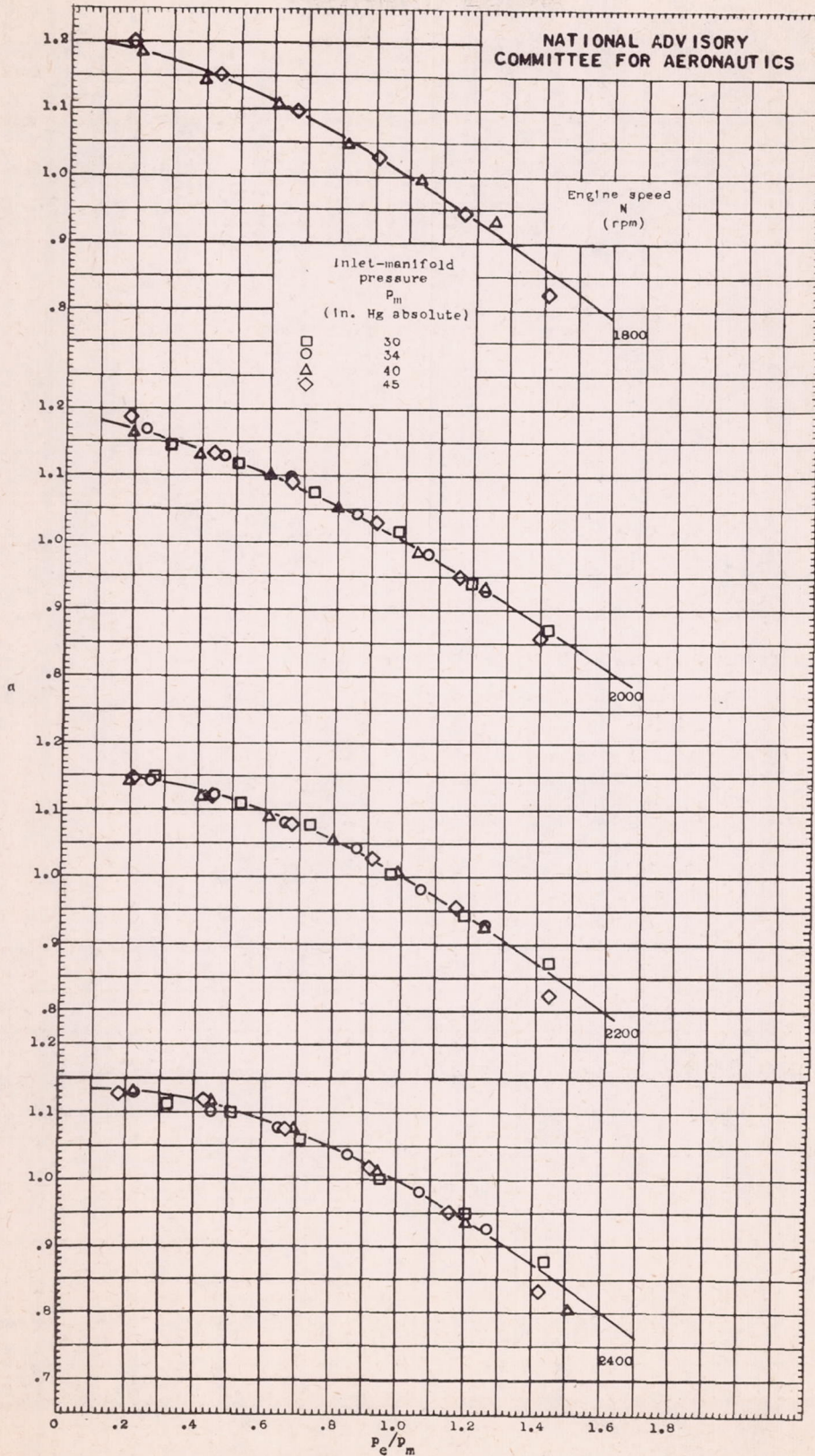
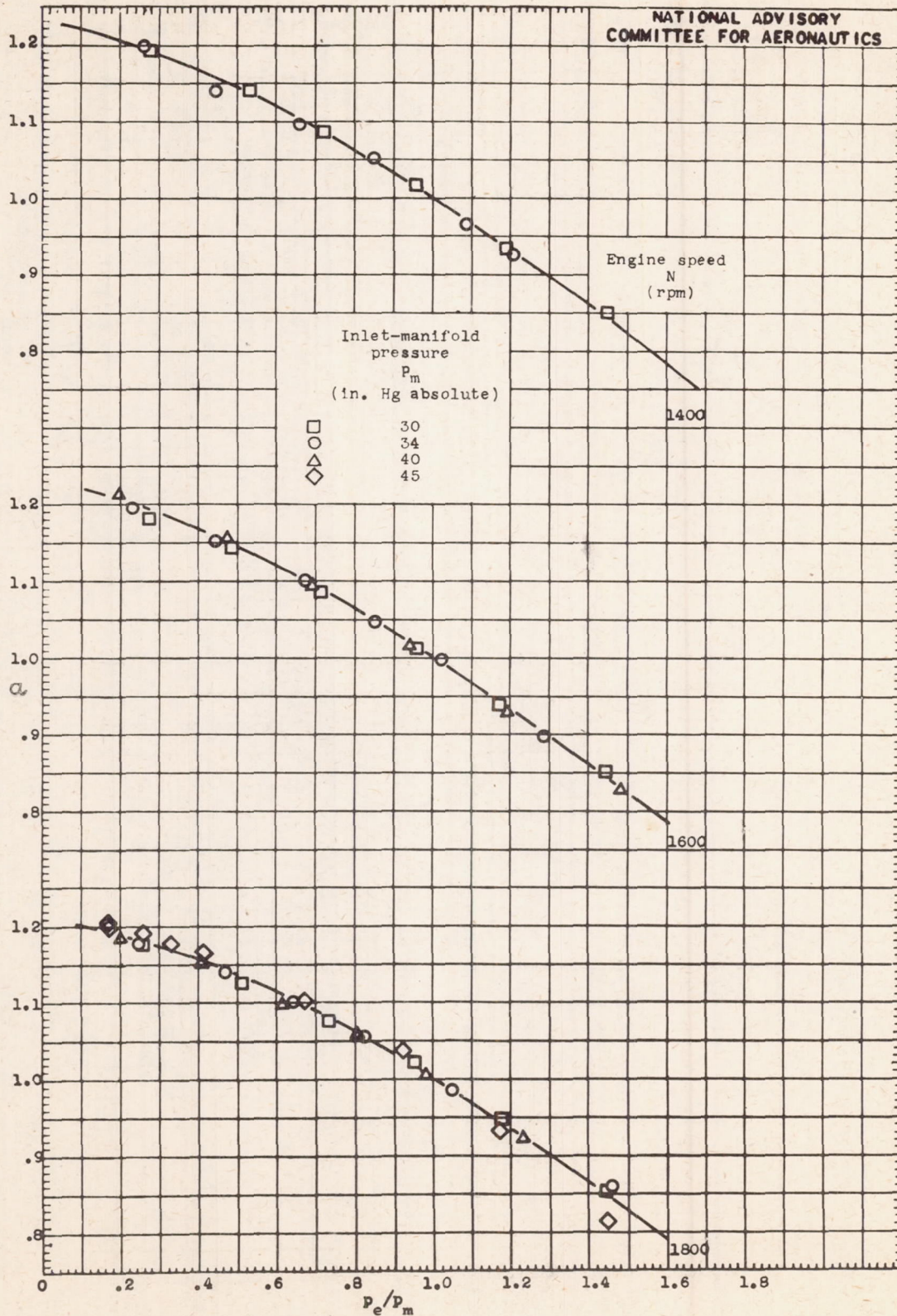
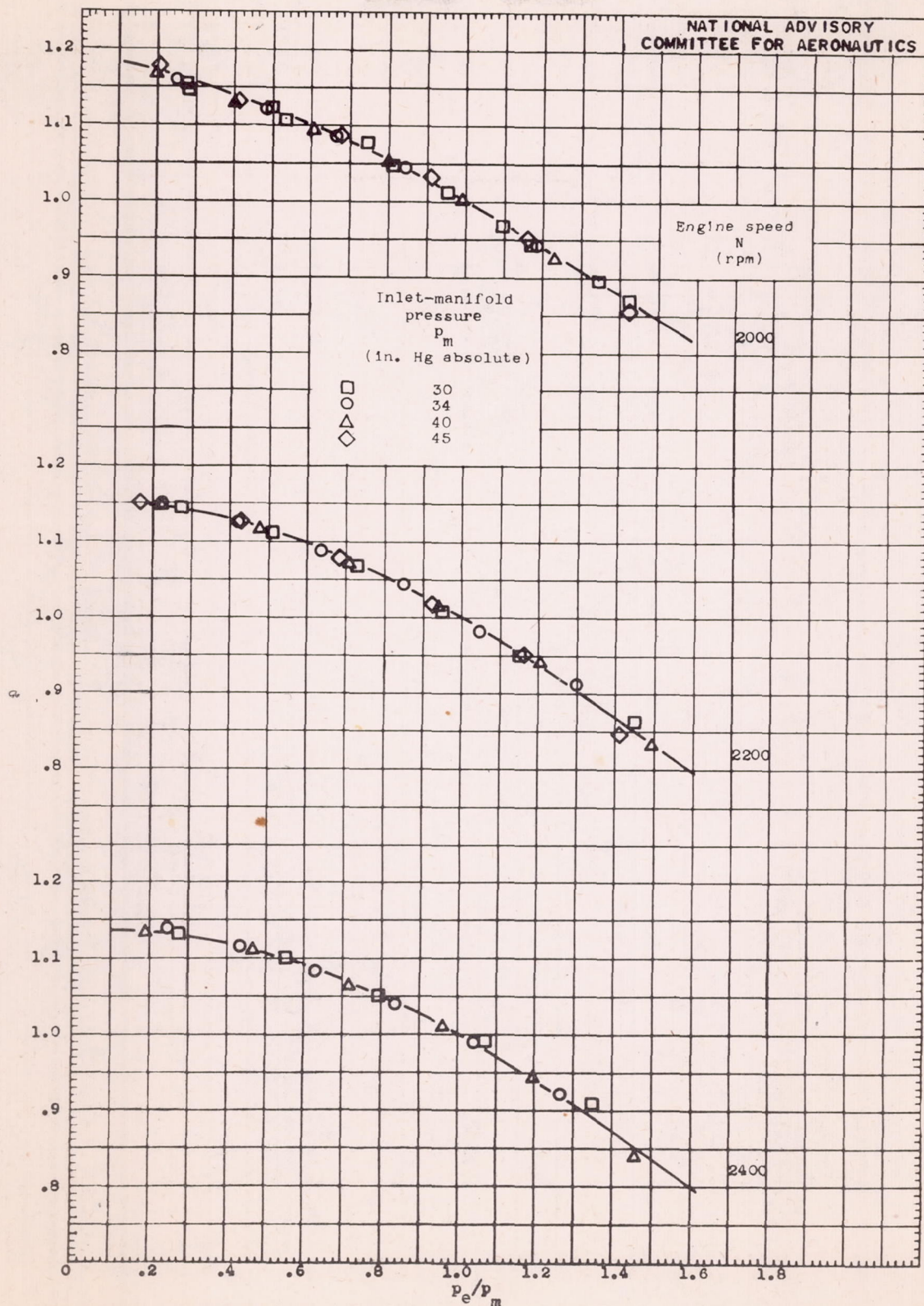


Figure 7. - Variation of α with p_e/p_m . Supercharger in low gear ratio (7.6 : 1).



(b) Fuel-air ratio, 0.085.

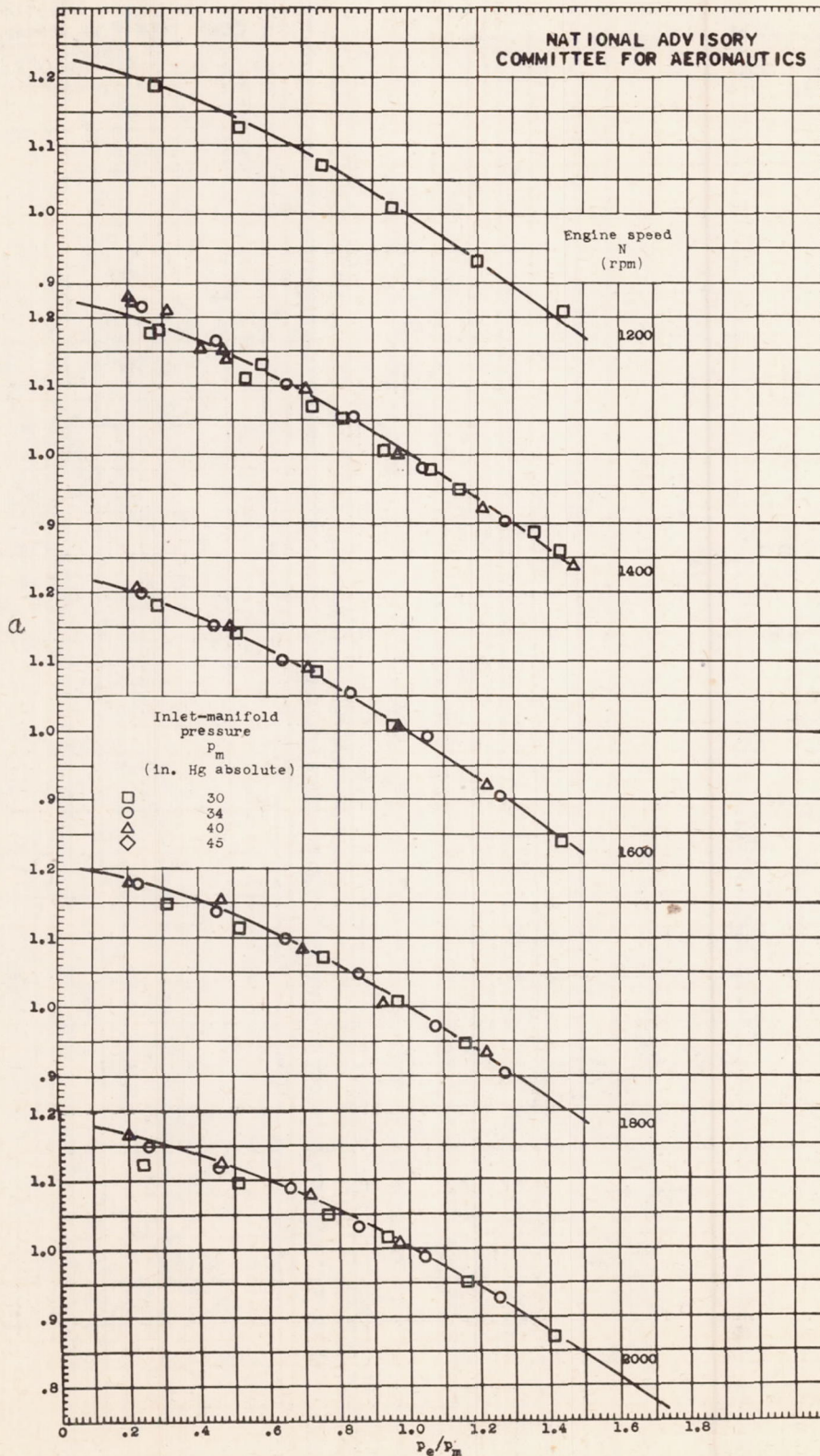
Figure 7. - Continued. Variation of α with P_e/P_m . Supercharger in low gear ratio (7.6 : 1).



(b) Concluded. Fuel-air ratio, 0.085.

Figure 7. - Continued. Variation of α with p_e/p_m . Supercharger in low gear ratio (7.6 : 1).

690



(c) Fuel-air ratio, 0.069.

Figure 7. - Concluded. Variation of α with p_e/p_m . Supercharger in low gear ratio (7.6 : 1).

690

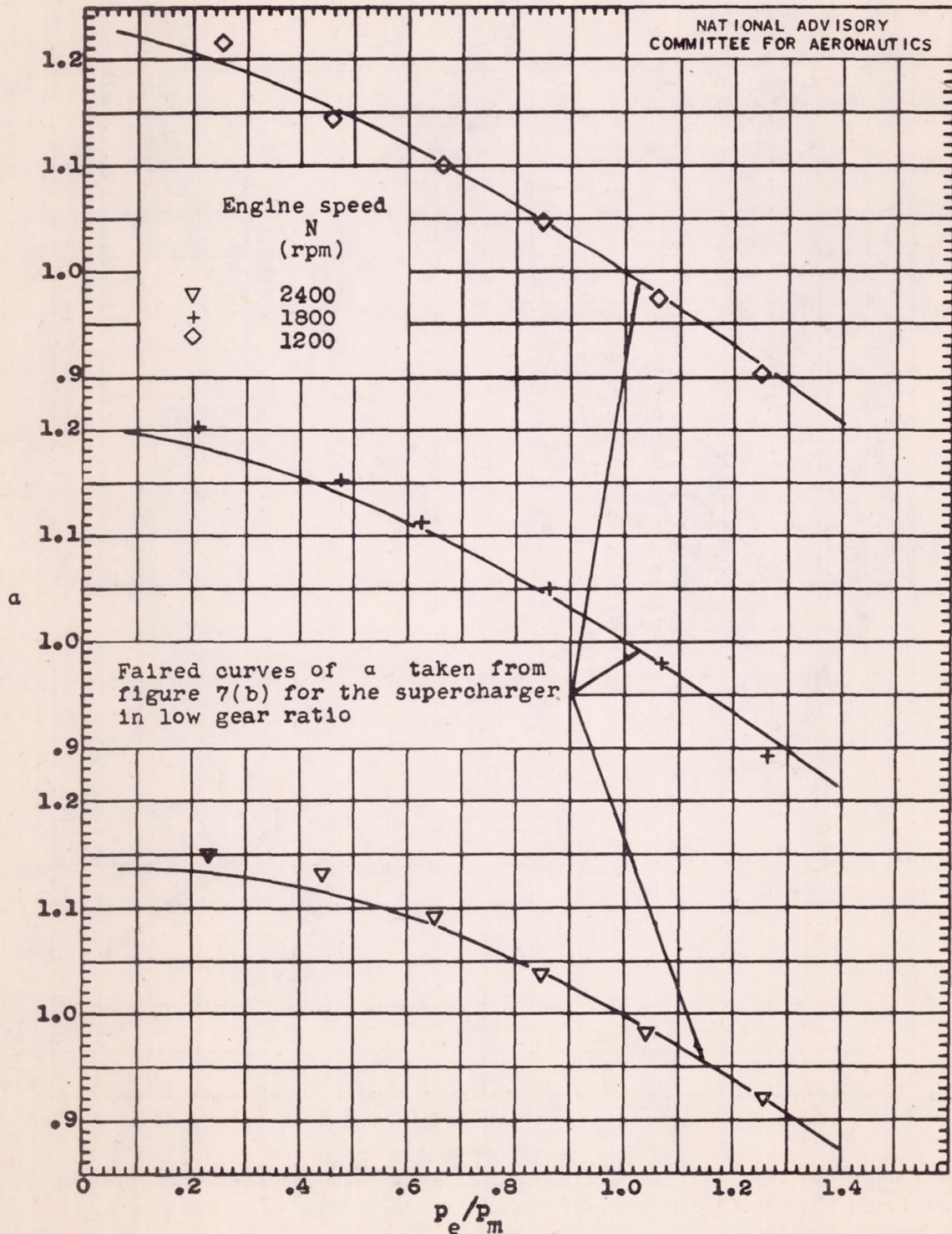


Figure 8. - Variation of α with P_e/P_m with supercharger in high gear ratio (9.45 : 1). Inlet-manifold pressure, 34 inches mercury absolute; fuel-air ratio, 0.085.

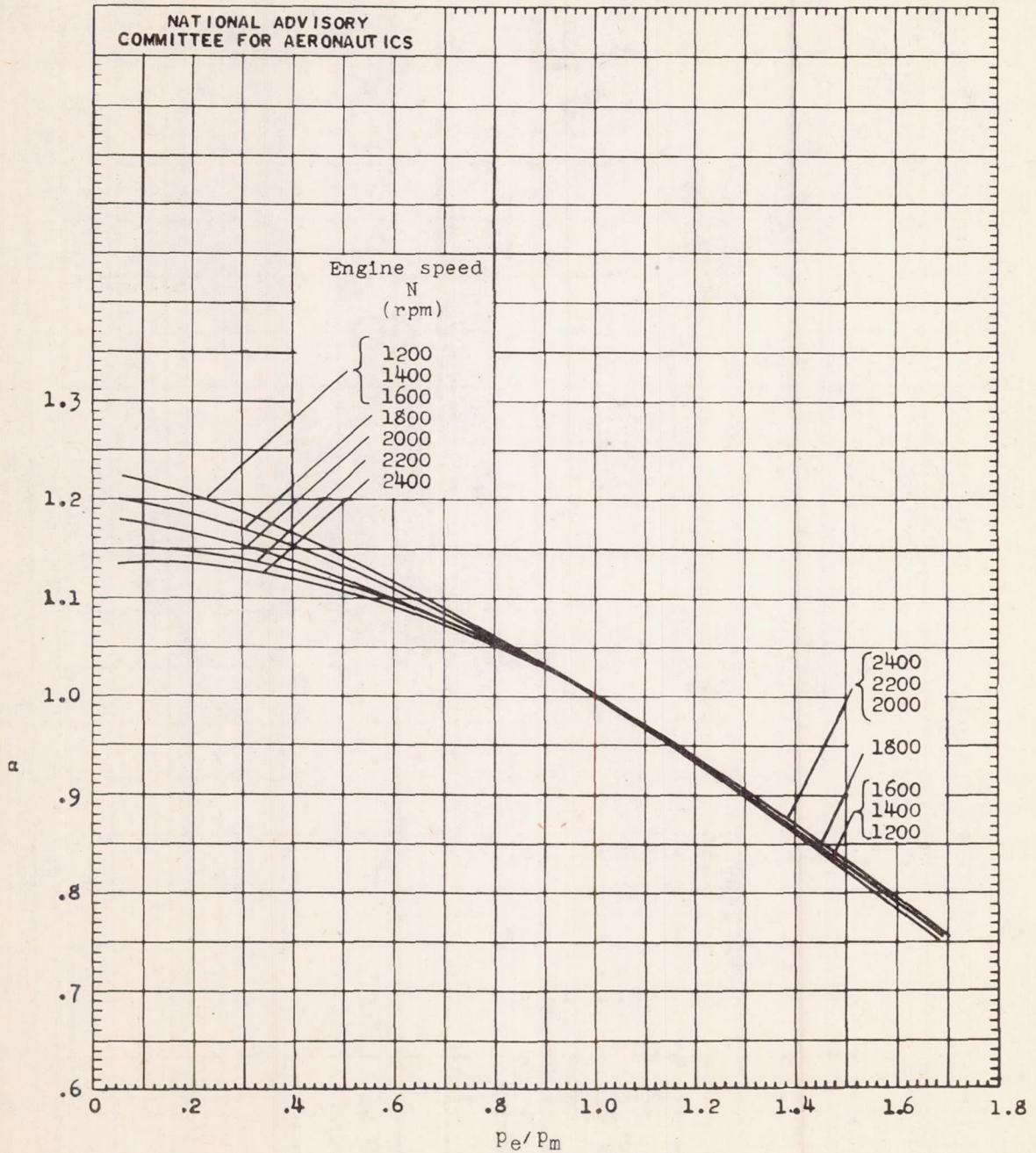


Figure 9. - Variation of α with p_e/p_m for various engine speeds, fuel-air ratios, inlet-manifold pressures, and for high and low gear ratio.

069

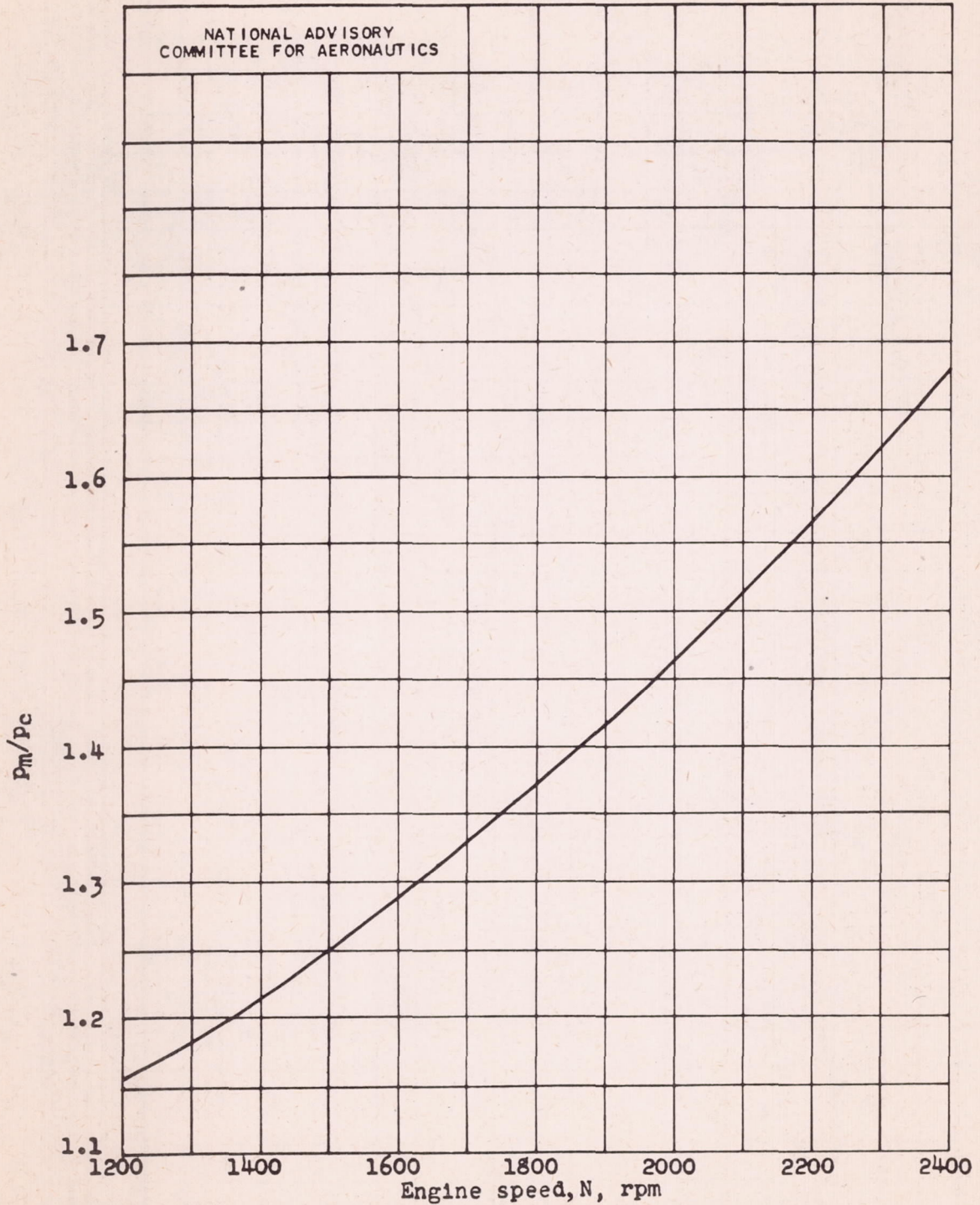
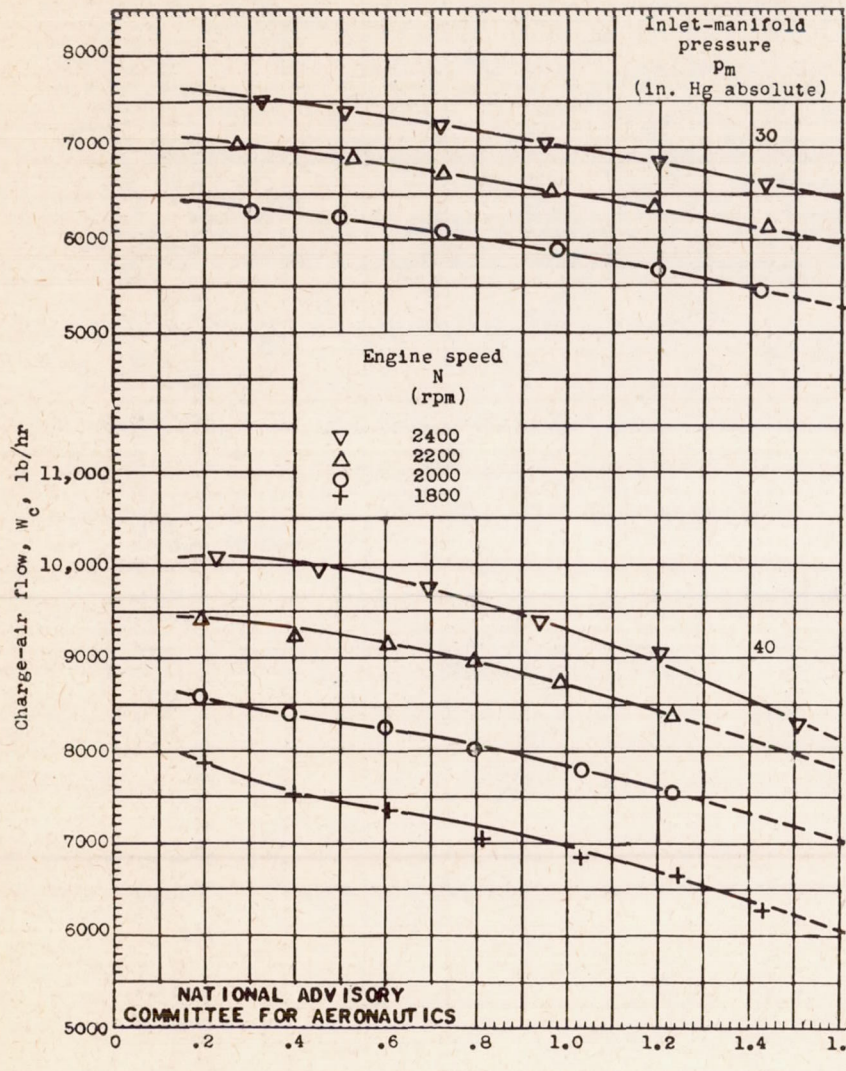


Figure 10. - Variation of ratio of inlet-manifold pressure to carburetor-inlet pressure P_m/P_c at full-open throttle with engine speed N . Carburetor-air temperature, $550^\circ R$.

690



(a) Fuel-air ratio, 0.100.

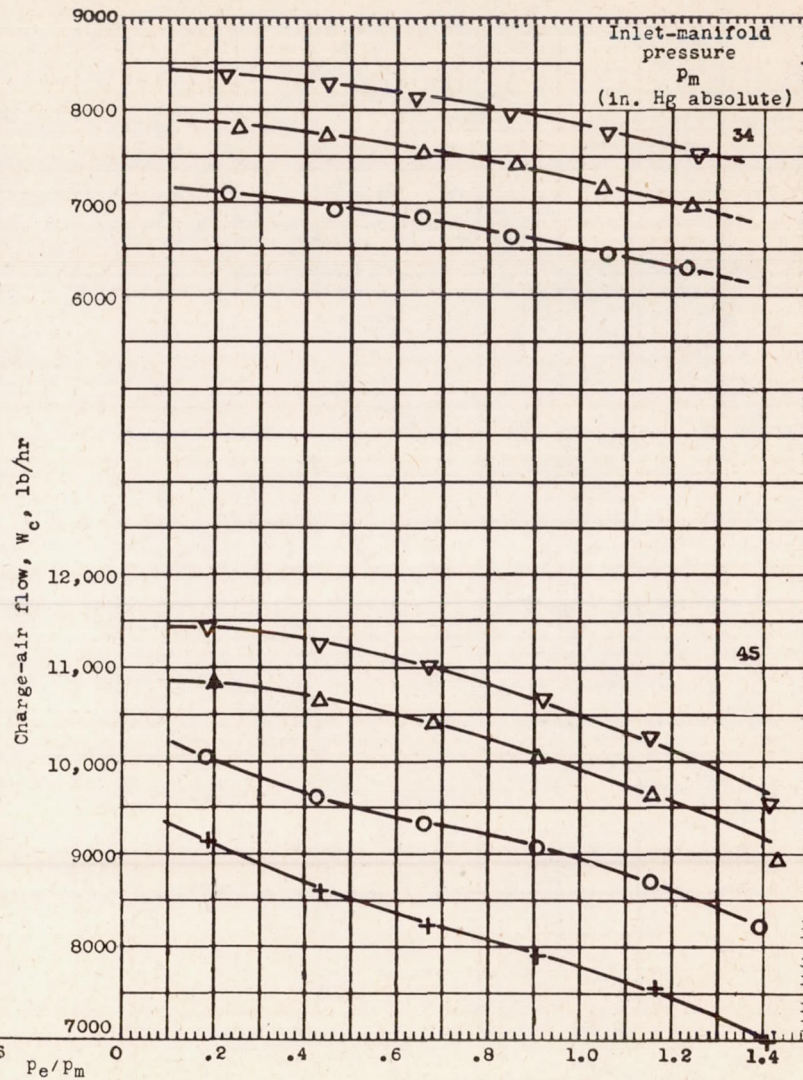
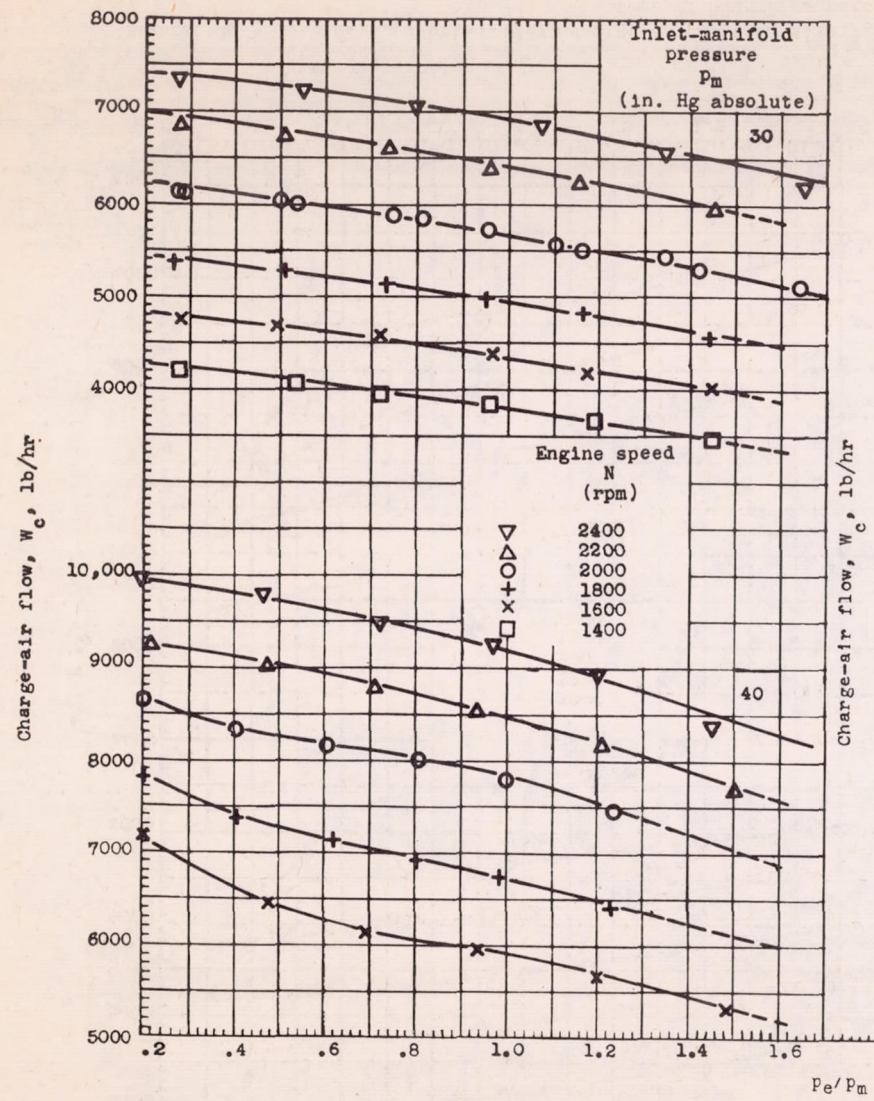
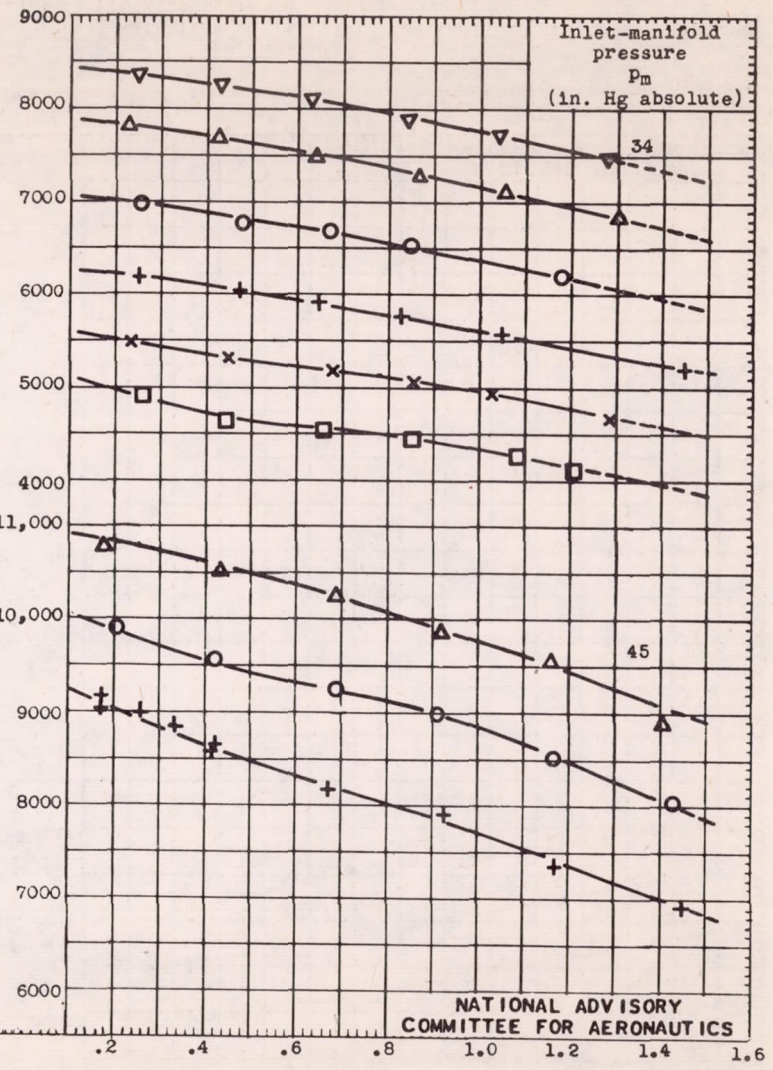


Figure 11. - Variation of charge-air flow W_c with p_e/p_m . Charge-air flow corrected to constant carburetor-air temperature of 550° R; supercharger in low gear ratio (7.6 : 1).

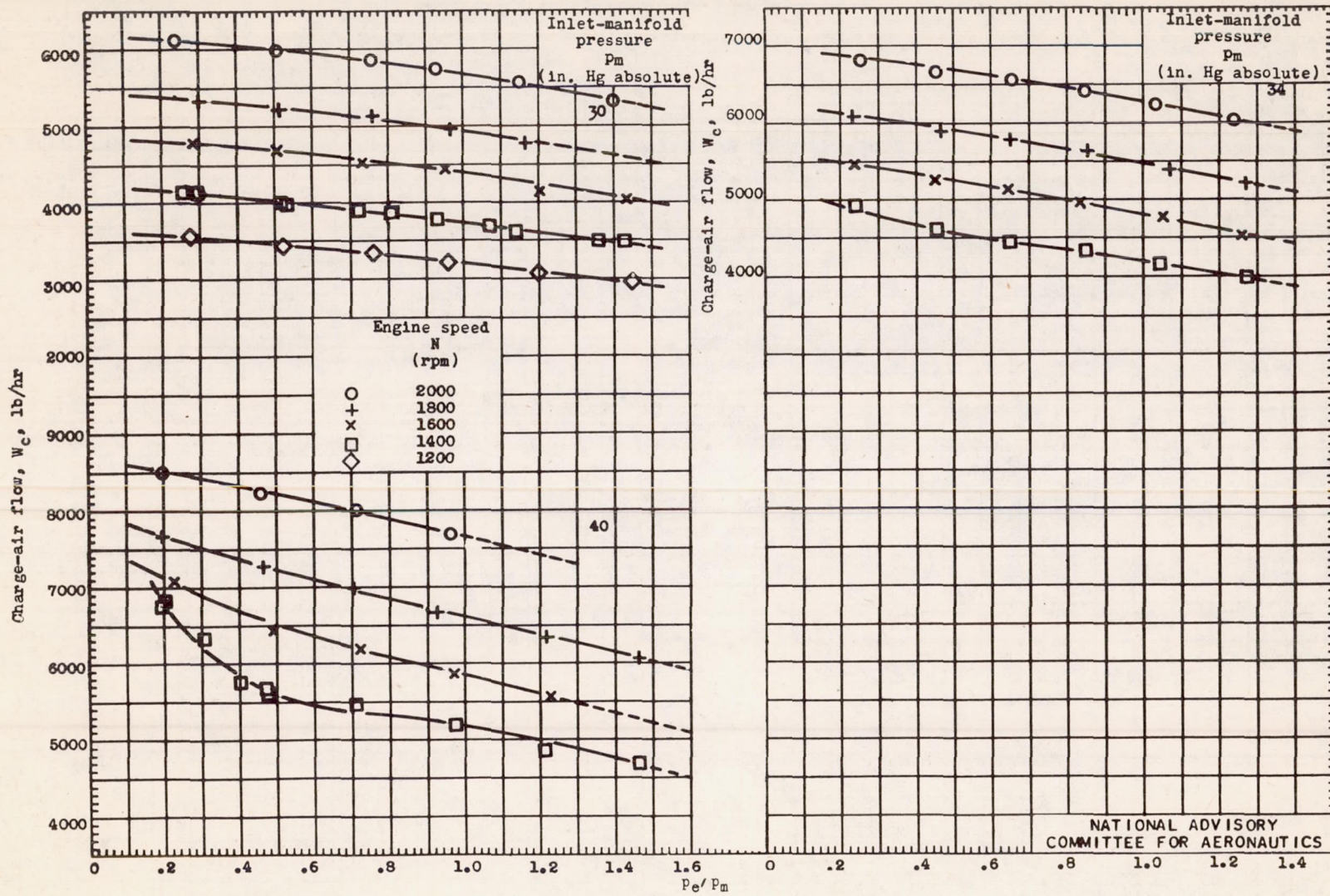


(b) Fuel-air ratio, 0.085.



NATIONAL ADVISORY
COMMITTEE FOR AERONAUTICS

Figure 11. - Continued. Variation of charge-air flow W_c with P_e/P_m . Charge-air flow corrected to constant carburetor-air temperature of 550° R; supercharger in low gear ratio (7.6 : 1).



(c) Fuel-air ratio, 0.069.

Figure 11. - Concluded. Variation of charge-air flow W_c with P_e/P_m . Charge-air flow corrected to constant carburetor-air temperature of 550° R; supercharger in low gear ratio (7.8 : 1).

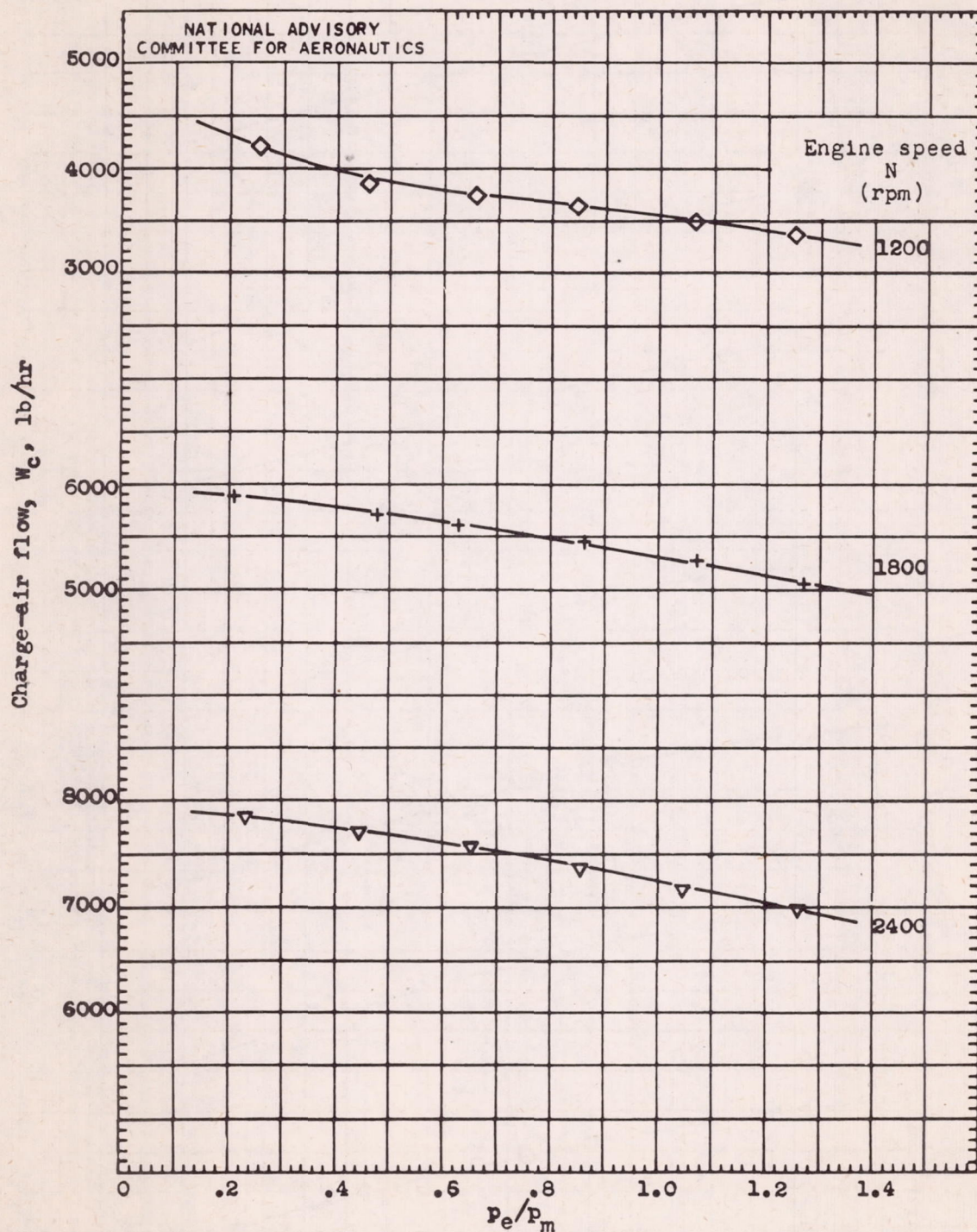
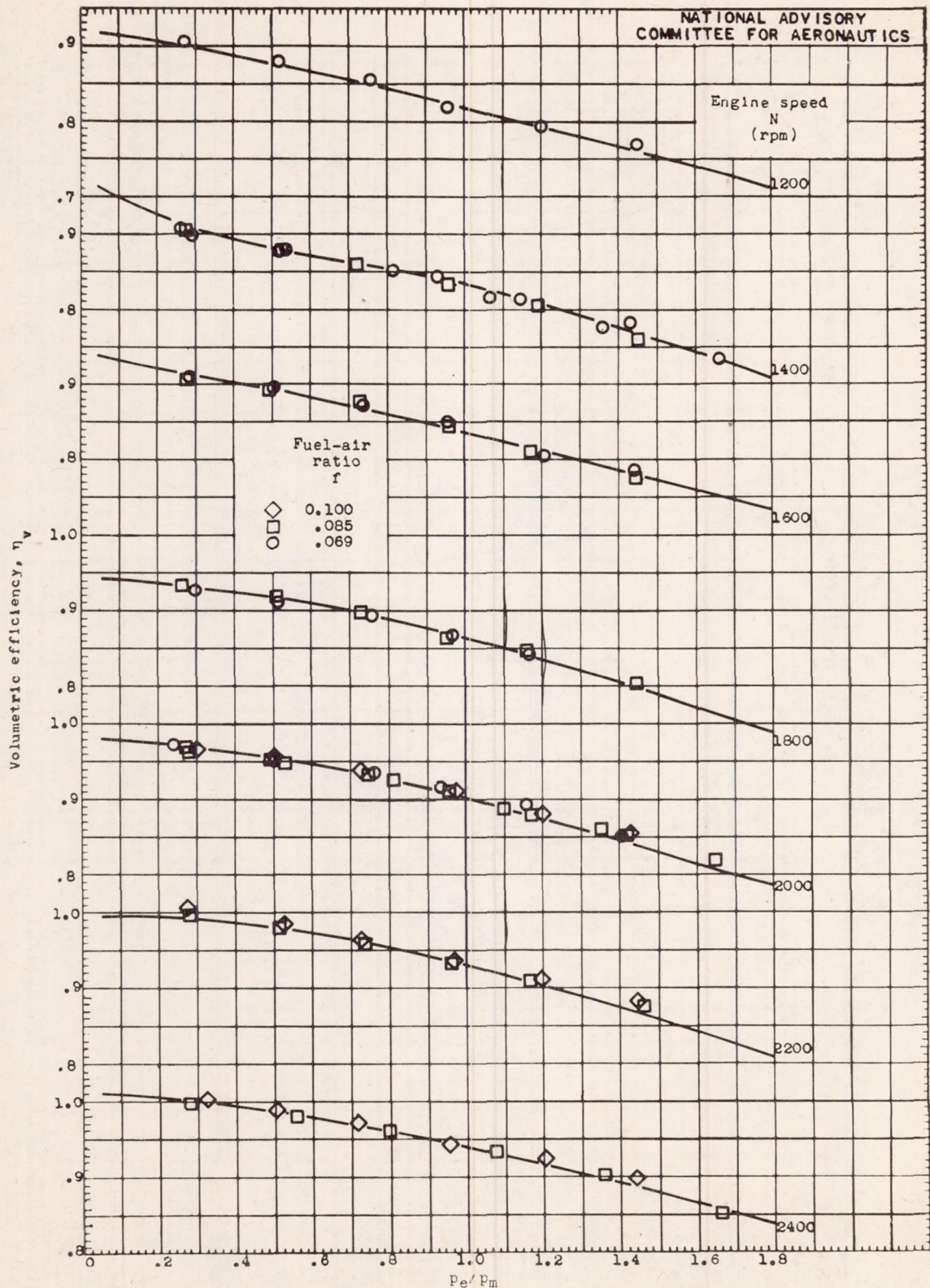


Figure 12. - Variation of charge-air flow W_c with p_e/p_m at constant inlet-manifold pressure of 34 inches mercury absolute and with supercharger in high gear ratio (9.45 : 1). Charge-air flow corrected to constant carburetor-air temperature of $550^\circ R$; fuel-air ratio, 0.085.

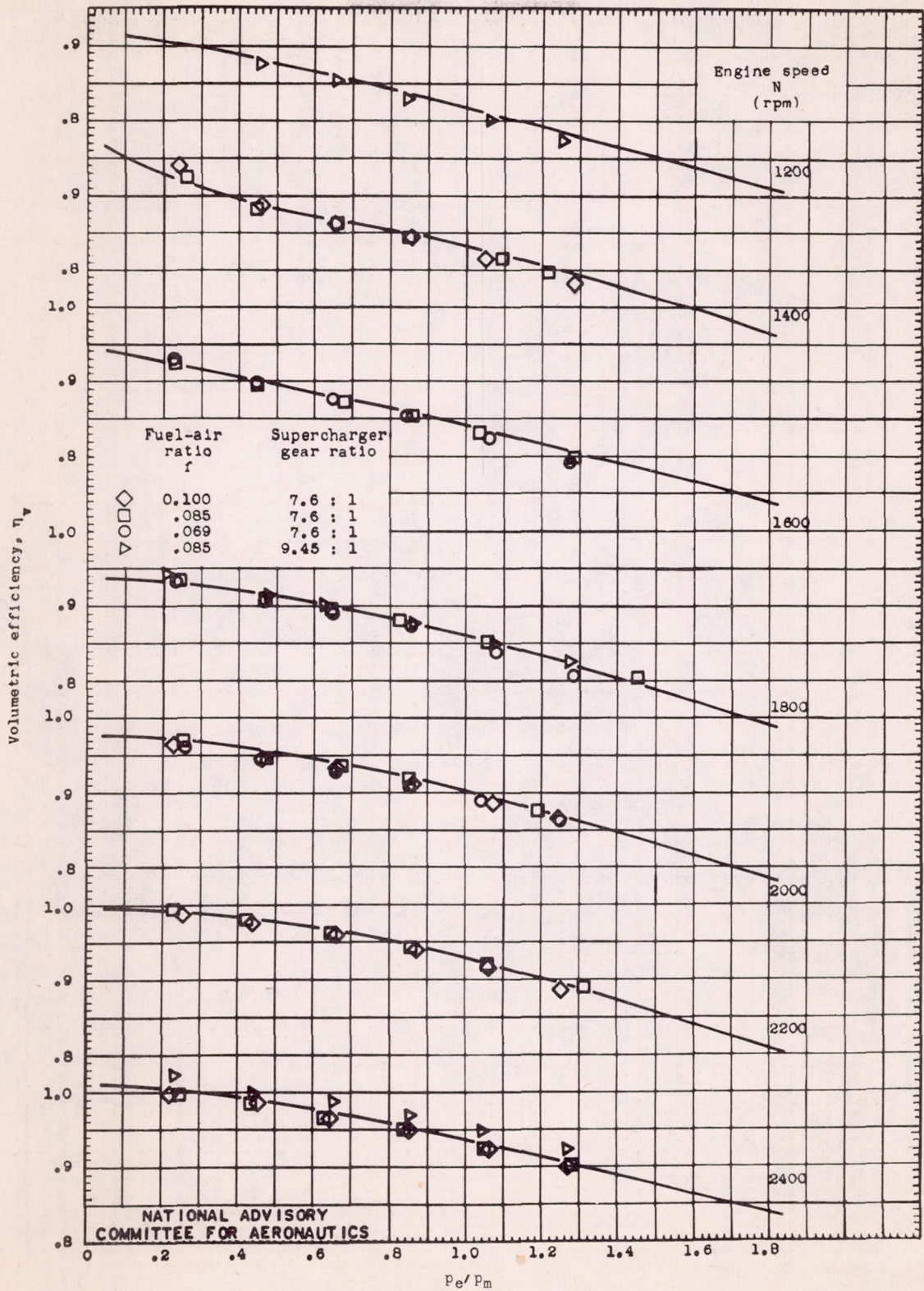
Fig. 13a



(a) Inlet-manifold pressure, 30 inches of mercury absolute.

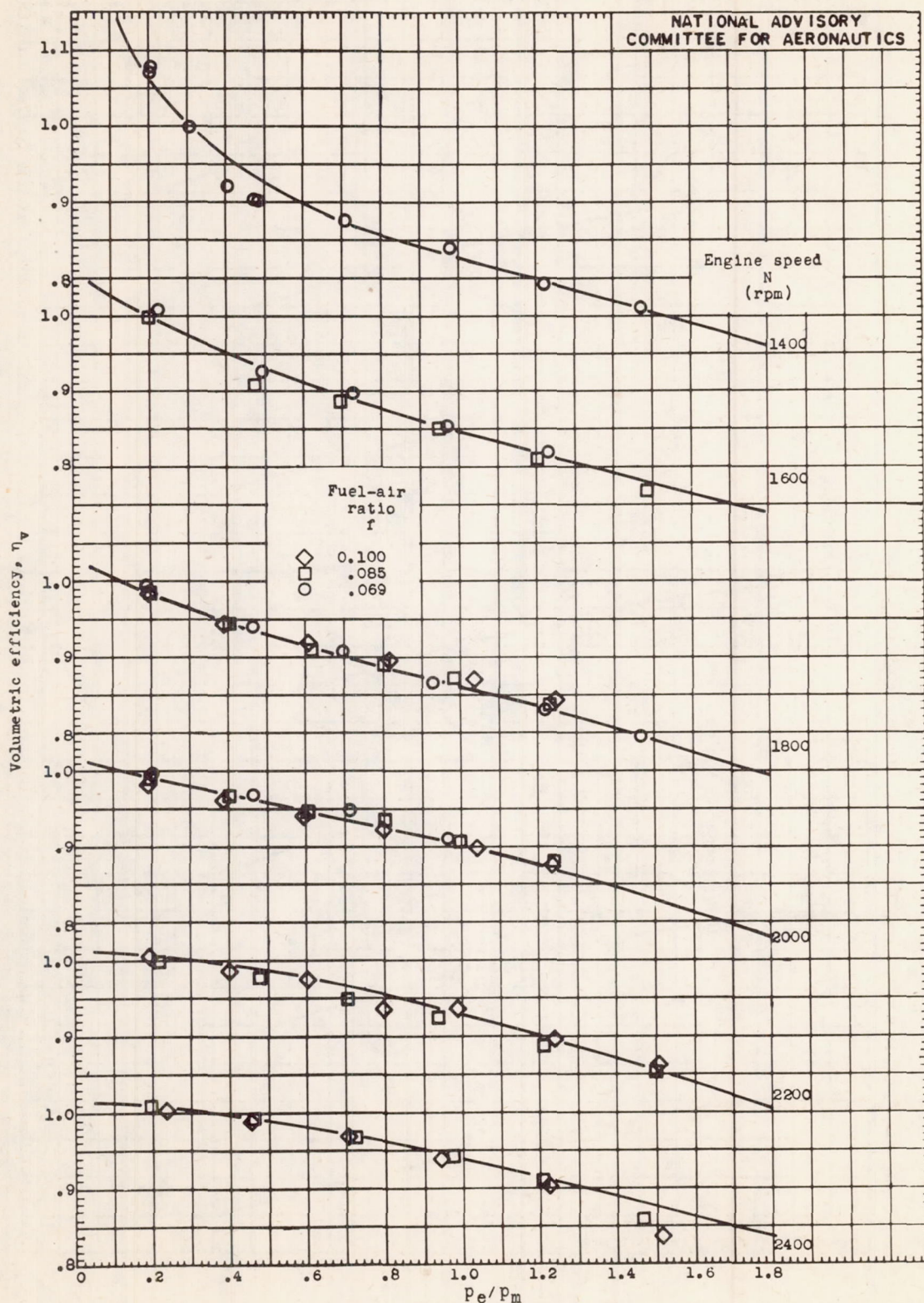
Figure 13. - Variation of volumetric efficiency η_v with p_e/p_m . Supercharger in low gear ratio (7.6 : 1) except where otherwise noted.

069



(b) Inlet-manifold pressure, 34 inches of mercury absolute.

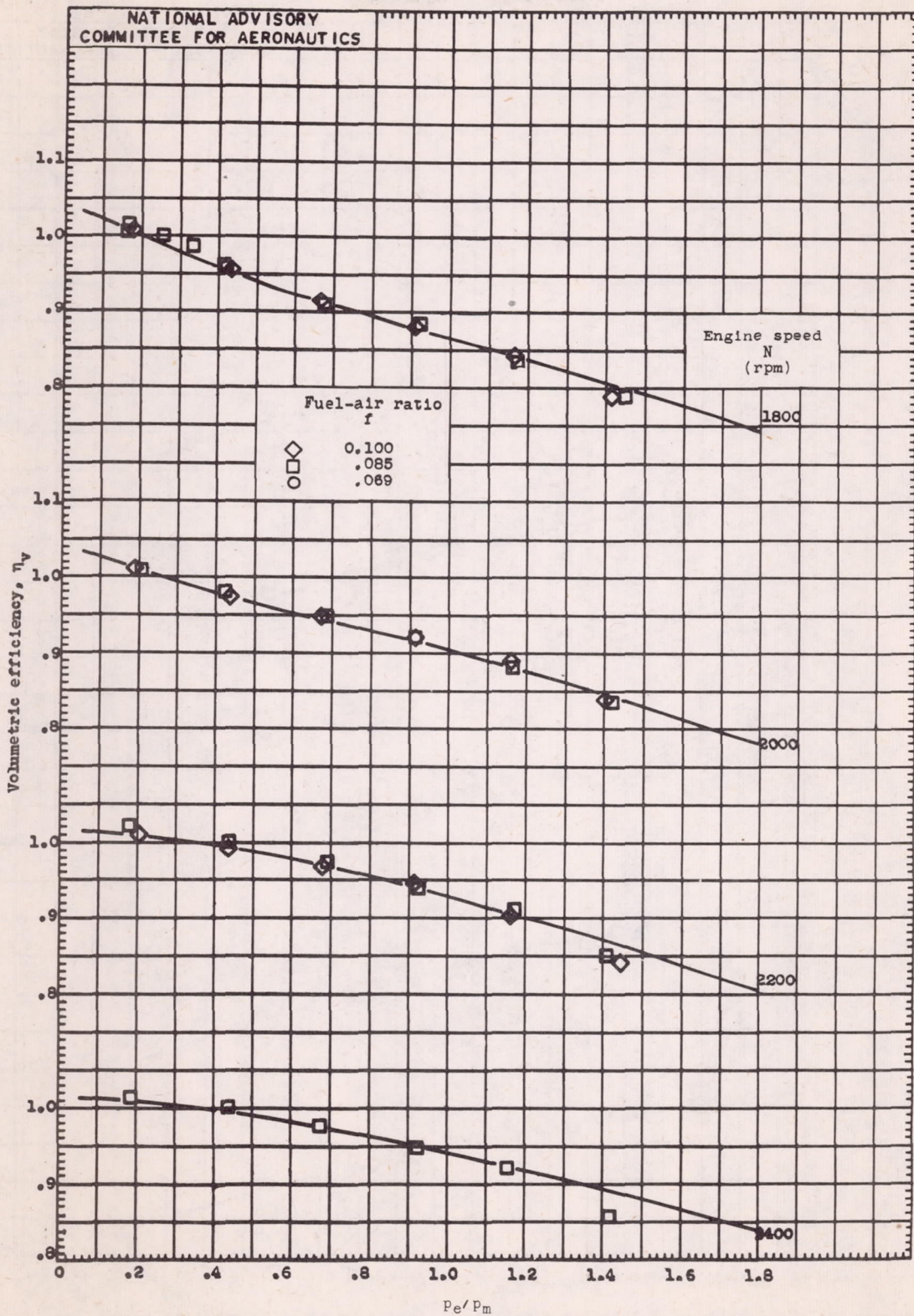
Figure 13. - Continued. Variation of volumetric efficiency η_v with p_e/p_m . Supercharger in low gear ratio (7.6 : 1) except where otherwise noted.



(c) Inlet-manifold pressure, 40 inches of mercury absolute.

Figure 13. - Continued. Variation of volumetric efficiency η_v with P_e/P_m . Supercharger in low gear ratio (7.6 : 1) except where otherwise noted.

069



(d) Inlet-manifold pressure, 45 inches of mercury absolute.

Figure 13. - Concluded. Variation of volumetric efficiency η_v with P_e/P_m . Supercharger in low gear ratio (7.6 : 1) except where otherwise noted.

690

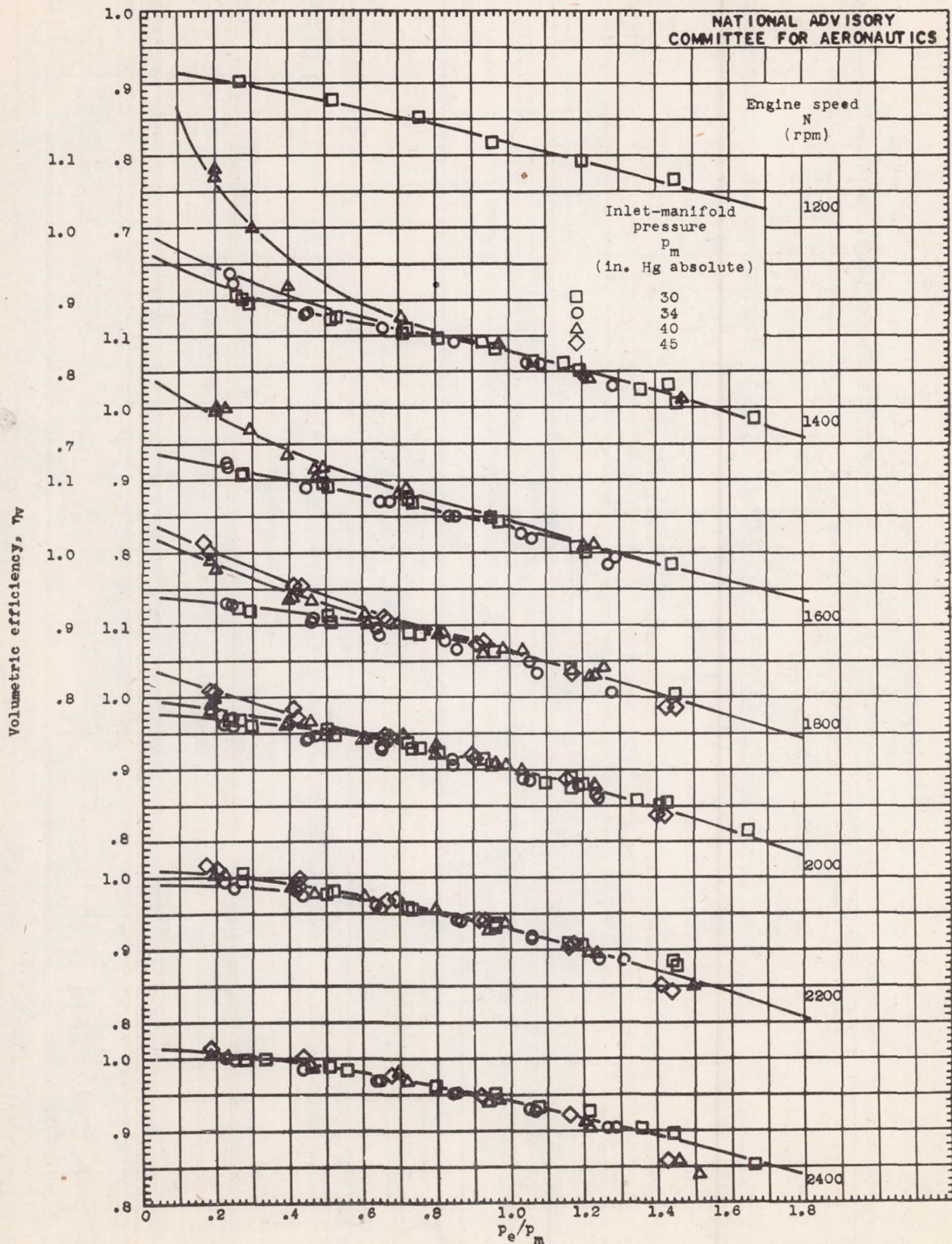


Figure 14. - Variation of volumetric efficiency η_v with p_e/p_m for constant engine speeds, inlet-manifold pressures, and three fuel-air ratios. Supercharger in low gear ratio (7.6 : 1).

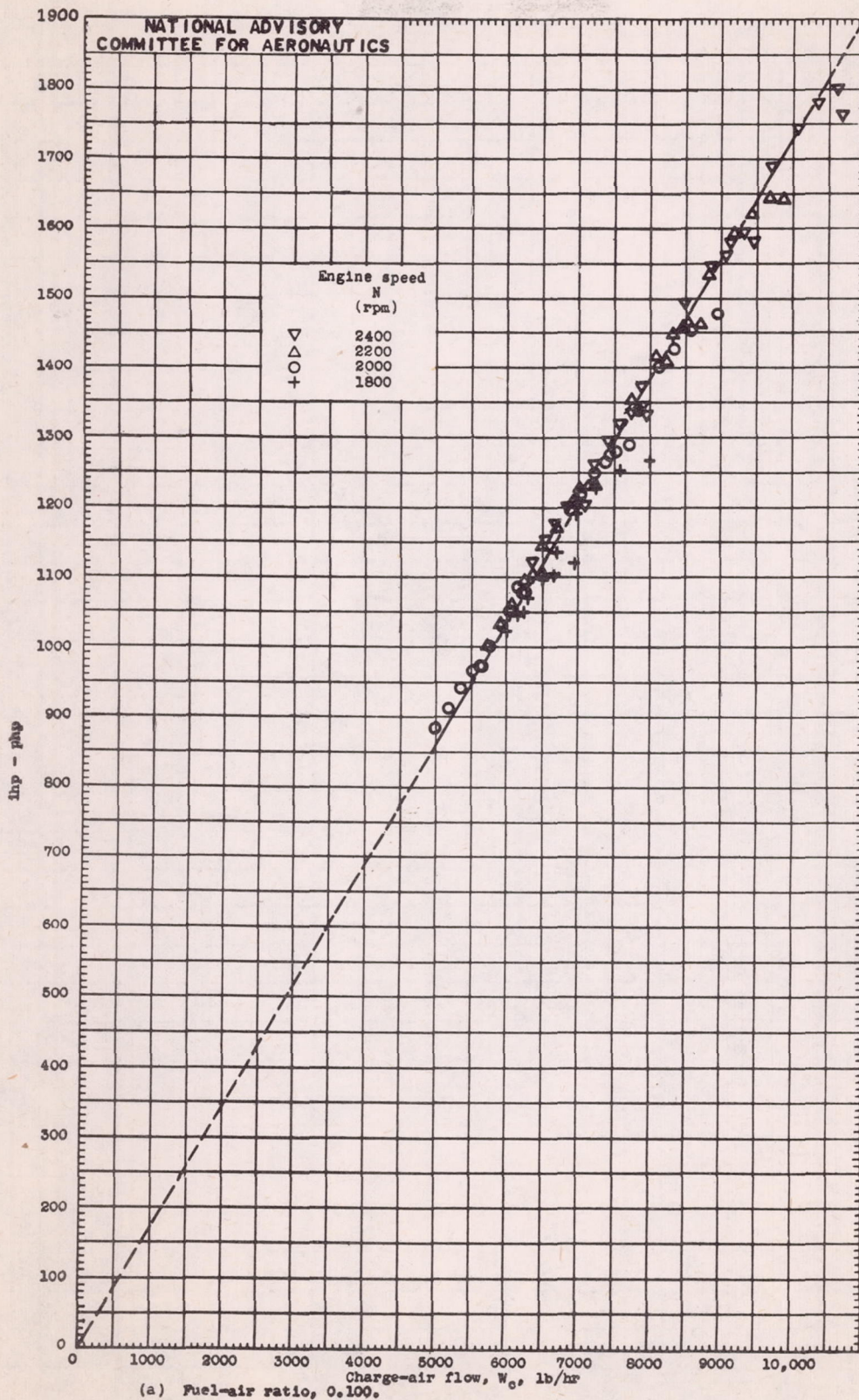
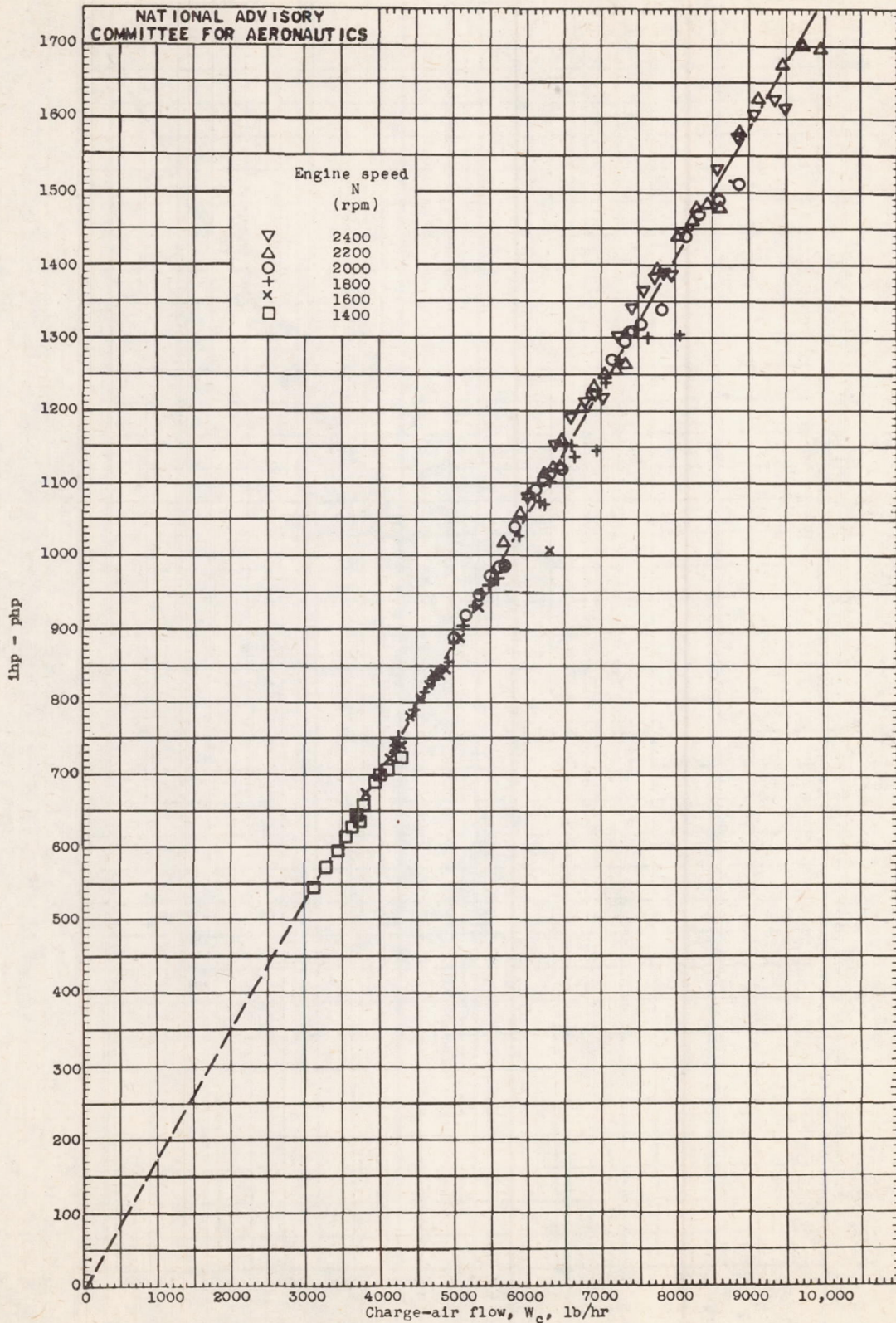
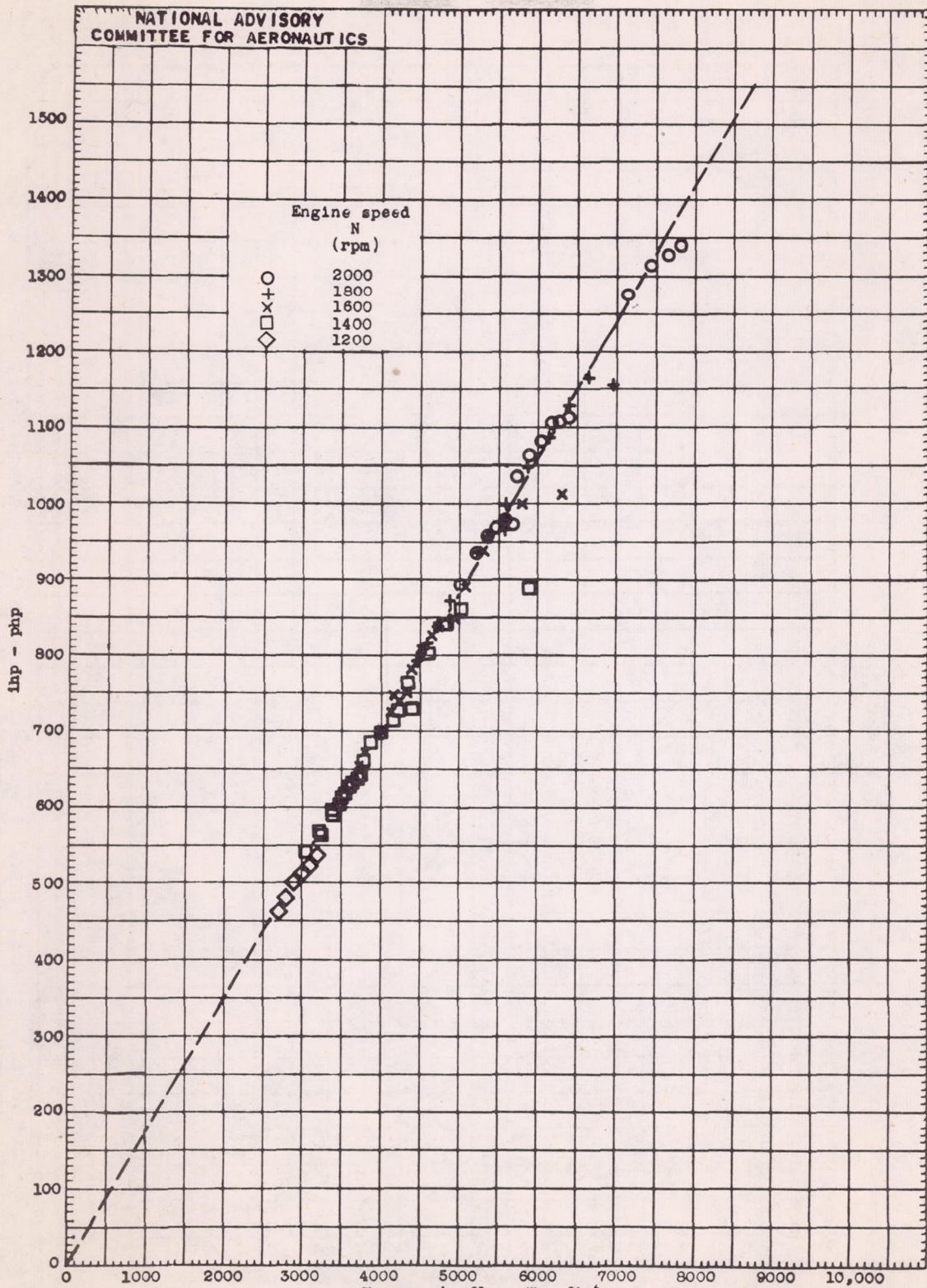


Figure 15. - Variation of $ihp - php$ with charge-air flow for various engine speeds and values of p_e/p_m . Charge-air flow W_c and $ihp - php$ corrected to a constant inlet-manifold mixture temperature T_m of $660^\circ R$; supercharger in low gear ratio (7.6 : 1).



(b) Fuel-air ratio, 0.085.

Figure 15. - Continued. Variation of ihp - php with charge-air flow for various engine speeds and values of p_e/p_m . Charge-air flow W_c and ihp - php corrected to a constant inlet-manifold mixture temperature T_m of $660^\circ R$; supercharger in low gear ratio (7.6 : 1).



(c) Fuel-air ratio, 0.069.

Figure 15. - Concluded. Variation of $ihp - php$ with charge-air flow for various engine speeds and values of p_e/p_m . Charge-air flow W_c and $ihp - php$ corrected to a constant inlet-manifold mixture temperature T_m of $660^\circ R$; supercharger in low gear ratio (7.6 : 1).

690

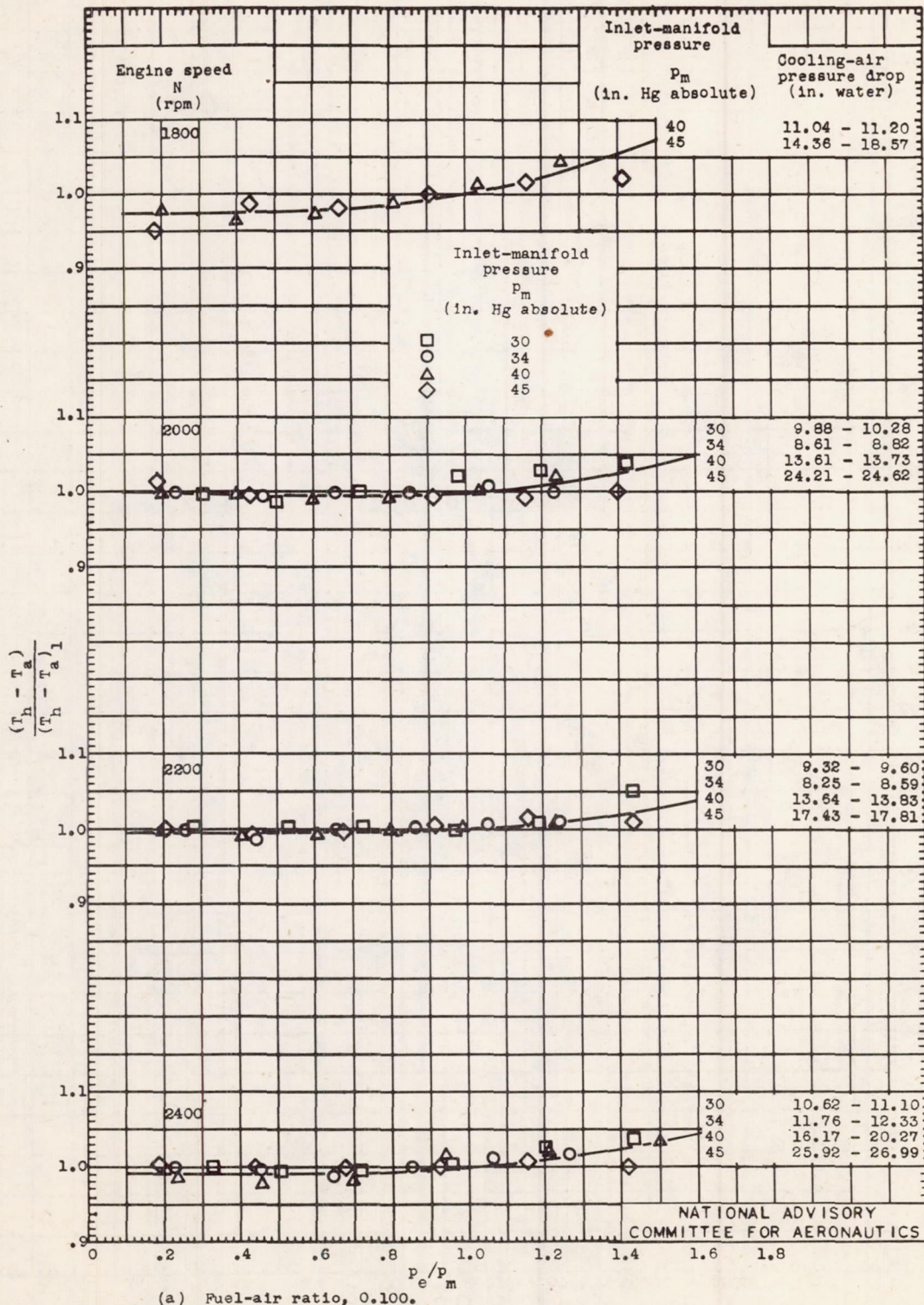


Figure 16. - Variation of $\frac{(T_h - T_a)}{(T_h - T_a)_1}$ with p_e/p_m for constant engine speeds, fuel-air ratios, inlet-manifold pressures, and cooling-air pressure drops. Supercharger in low gear ratio (7.6 : 1).

069

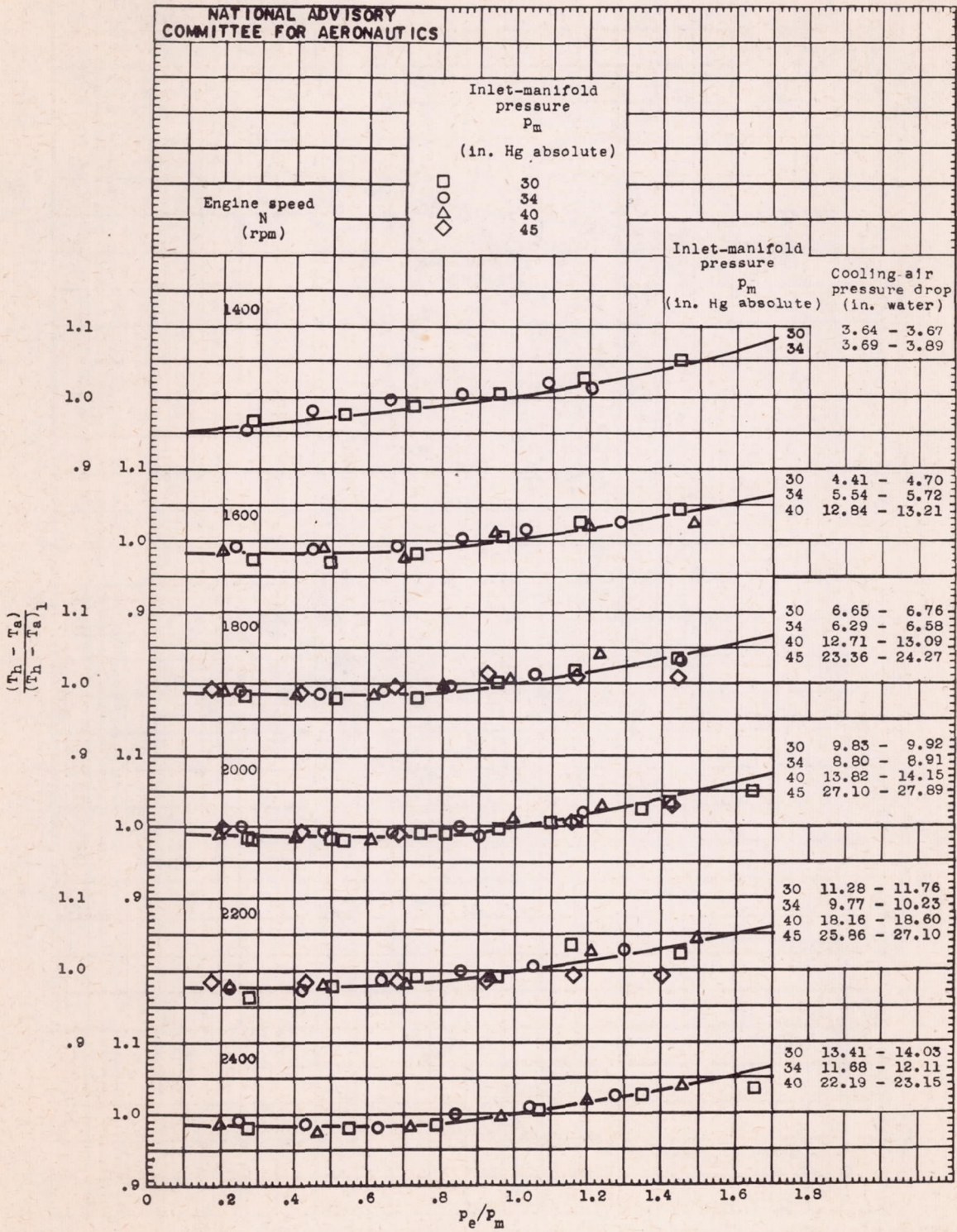


Figure 16. - Continued. Variation of $\frac{(T_h - T_a)}{(T_h - T_a)_1}$ with p_e/p_m for constant engine speeds, fuel-air ratios, inlet-manifold pressures, and cooling-air pressure drops. Supercharger in low gear ratio (7.6 : 1).

690

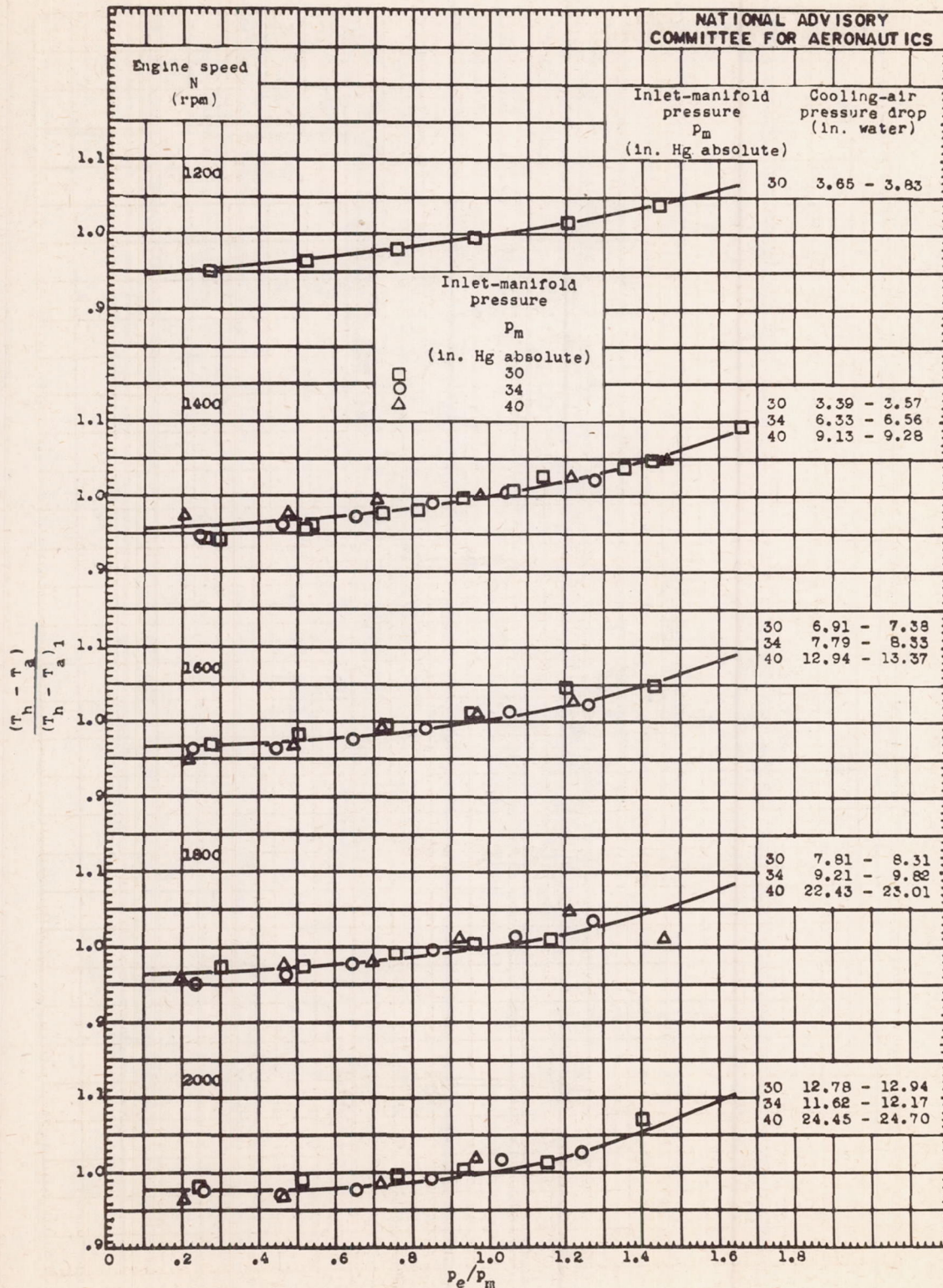


Figure 16. - Concluded. Variation of $\frac{(T_h - T_a)}{(T_h - T_a)_1}$ with p_e/p_m for constant engine speeds, fuel-air ratios, inlet-manifold pressures, and cooling-air pressure drops. Supercharger in low gear ratio (7.6 : 1).

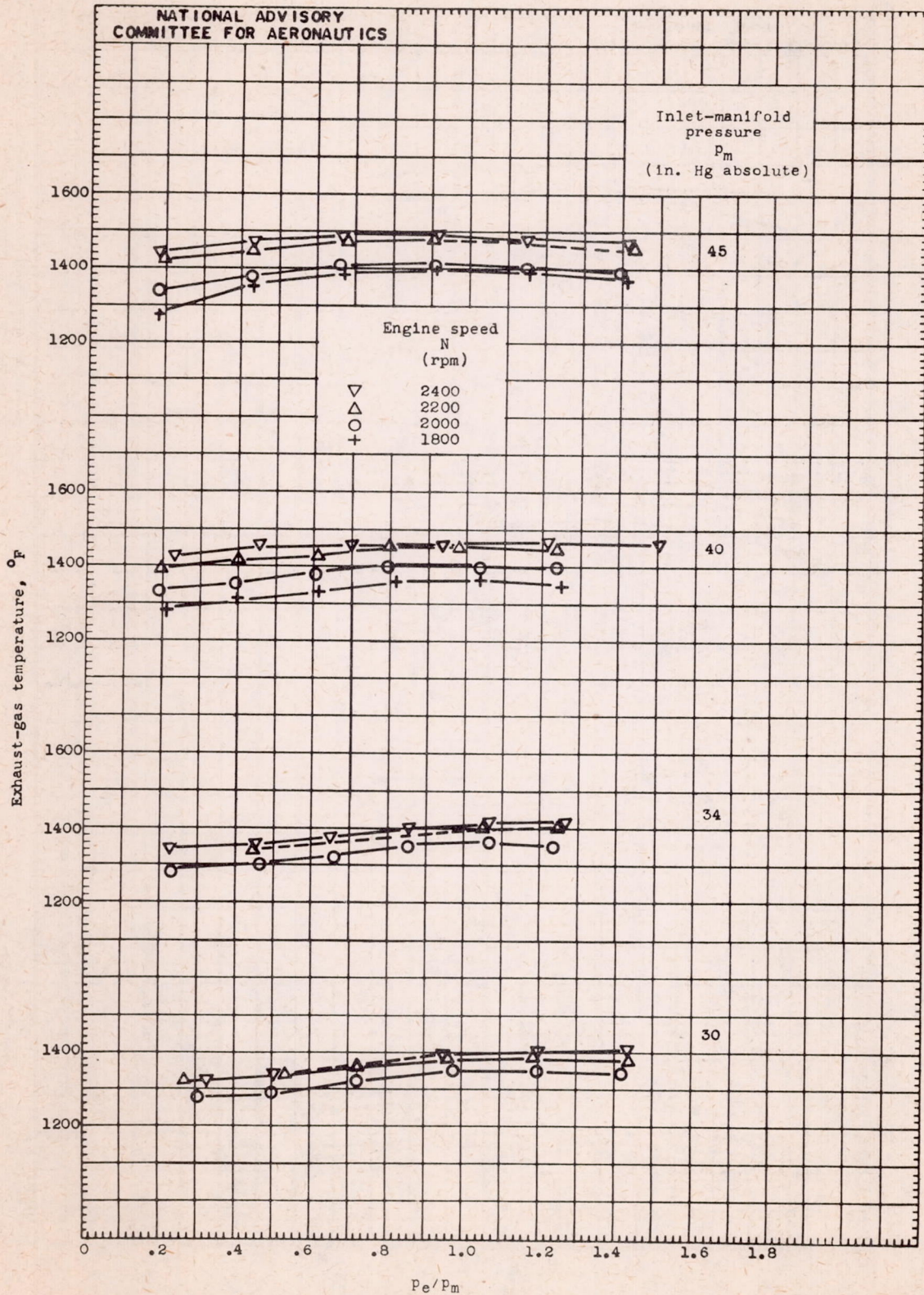


Figure 17. - Variation of exhaust-gas temperature with p_e/p_m for constant engine speeds, inlet-manifold pressures, and fuel-air ratios. Supercharger in low gear ratio (7.6 : 1).

690

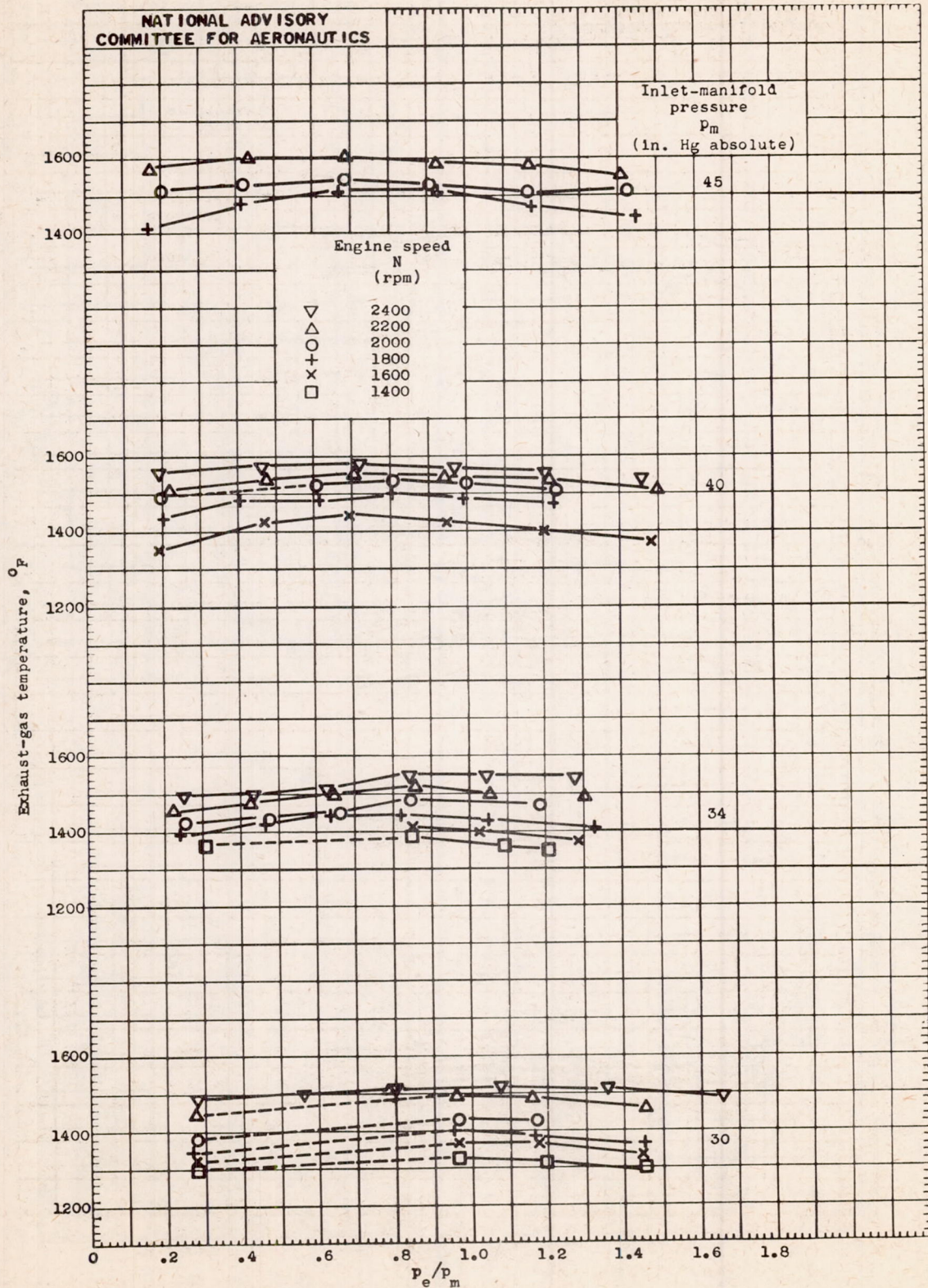
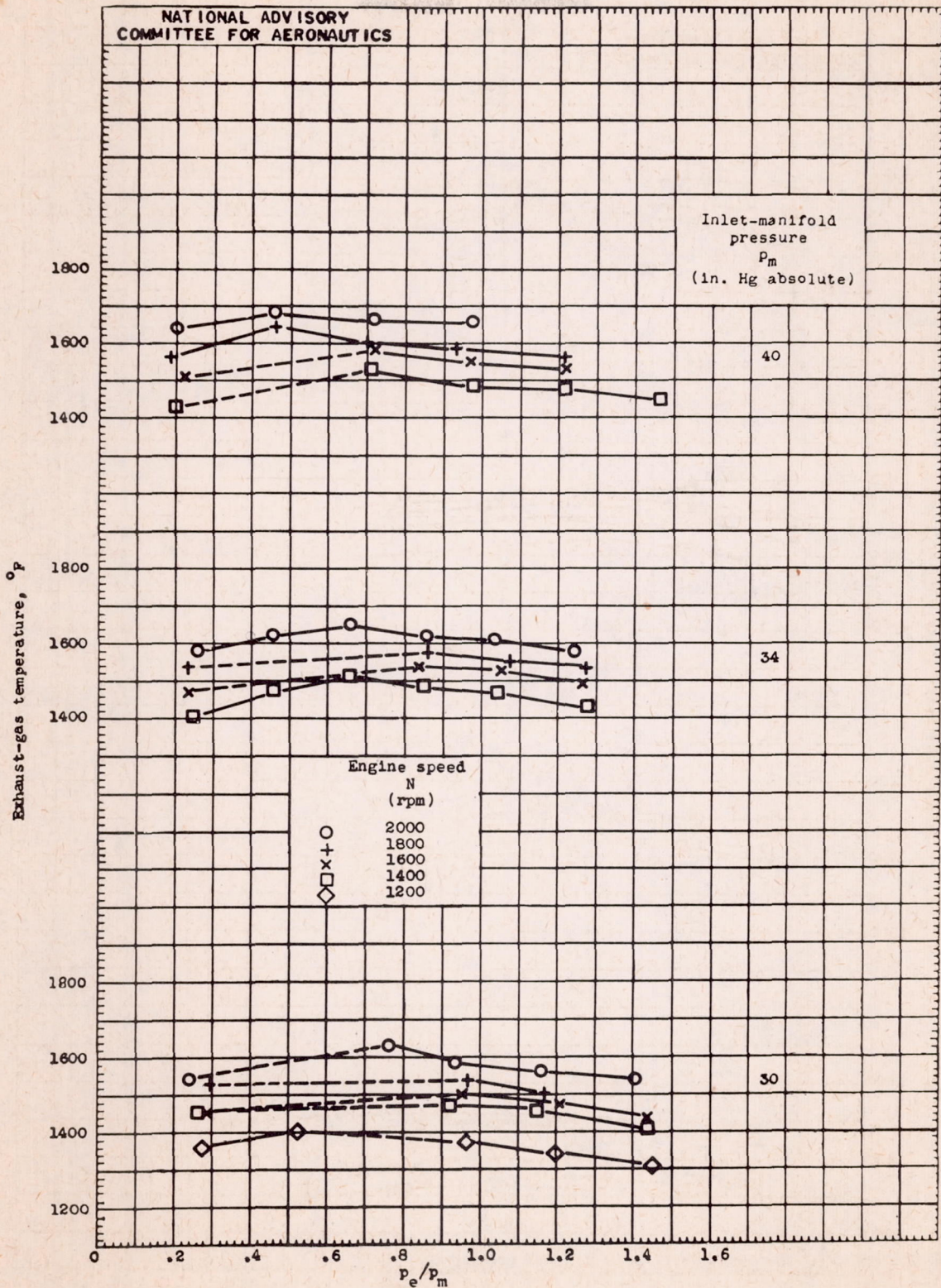


Figure 17. - Continued. Variation of exhaust-gas temperature with p_e/p_m for constant engine speeds, inlet-manifold pressures, and fuel-air ratios. Supercharger in low gear ratio (7.6 : 1).

069



(c) Fuel-air ratio, 0.069.

Figure 17. - Concluded. Variation of exhaust-gas temperature with p_e/p_m for constant engine speeds, inlet-manifold pressures, and fuel-air ratios. Supercharger in low gear ratio (7.6 : 1).

690

